Author Manuscript

Author Manuscript

Author Manuscript

Author Manuscript

HHS Public Access

Author manuscript

Stem Cells. Author manuscript; available in PMC 2016 August 01.

Published in final edited form as:

Stem Cells. 2015 August ; 33(8): 2400–2415. doi:10.1002/stem.2053.

Mesenchymal Stem Cells Isolated from Human Gliomas Increase Proliferation and Maintain Stemness of Glioma Stem Cells Through the IL-6/gp130/STAT3 pathway

Anwar Hossain[1,7], **Joy Gumin**[1,7], **Feng Gao**[1,7], **Javier Figueroa**[1,7], **Naoki Shinojima**[1,7], **Tatsuya Takezaki**[1,7], **Waldemar Priebe**[2,7], **Diana Villarreal**[1,7], **Seok-Gu Kang**[1,7], **Celine Joyce**[1,7], **Erik Sulman**[3,7], **Qianghu Wang**[4,7], **Frank C. Marini**[8], **Michael Andreeff**[5], **Howard Colman**[9], and **Frederick F. Lang**[1,7]

[1]Department of Neurosurgery, The University of Texas M.D. Anderson Cancer Center, Houston, TX 77030

[2]Department of Experimental Therapeutics, The University of Texas M.D. Anderson Cancer Center, Houston, TX 77030

[3]Department of Radiation Oncology, The University of Texas M.D. Anderson Cancer Center, Houston, TX 77030

[4]Department of Bioinformatics and Computational Biology, The University of Texas M.D. Anderson Cancer Center, Houston, TX 77030

[5]Department of Leukemia, The University of Texas M.D. Anderson Cancer Center, Houston, TX 77030

[6]Department of Pathology, The University of Texas M.D. Anderson Cancer Center, Houston, TX 77030

[7]The Brain Tumor Center, The University of Texas M.D. Anderson Cancer Center, Houston, TX 77030

Address Correspondence to: Frederick F. Lang, MD, Department of Neurosurgery – Unit 442, The University of Texas MD Anderson Cancer Center, 1400 Holcombe Blvd., Houston, TX 77030, Phone: 713-792-2400, Fax: 713-794-4950, flang@mdanderson.org.

Anwar Hossain: design, collection and assembly of data, data analysis and interpretation, manuscript writing, final approval of manuscript
Joy Gumin: collection and assembly of data
Feng Gao: collection and assembly of data
Javier Figueroa: collection and assembly of data
Naoki Shinojima: collection and assembly of data
Tatsuya Takezaki: collection and assembly of data
Waldemar Priebe: provision of study material
Diana Villarreal: collection and assembly of data
Seok-Gu Kang: collection and assembly of data
Celine Joyce: collection and assembly of data
Erik Sulman: provision of study material, collection and assembly of data, data analysis and interpretation
Qianghu Wang: data analysis and interpretation
Frank Marini: provision of study material
Michael Andreeff: provision of study material
Howard Colman: provision of study material
Frederick Lang: conception and design, financial support, administrative support, provision of study material and patients, data analysis and interpretation, manuscript writing, final approval of manuscript

Author Manuscript Author Manuscript Author Manuscript Author Manuscript

[8]Department of Cancer Biology, Wake Forest School of Medicine, Winston-Salem, NC 27157

[9]Department of Neuro-Oncology, University of Utah Health Science Center, Salt Lake City, UT 84132

Abstract

Although mesenchymal stem cells (MSCs) have been implicated as stromal components of several cancers, their ultimate contribution to tumorigenesis and their potential to drive cancer stem cells, particularly in the unique microenvironment of human brain tumors, remains largely undefined. Consequently, using established criteria, we isolated glioma-associated-human MSCs (GA-hMSCs) from fresh human glioma surgical specimens for the first time. We show that these GA-hMSCs are nontumorigenic stromal cells that are phenotypically similar to prototypical bone marrow-MSCs. Low-passage genomic sequencing analyses comparing GA-hMSCs with matched tumor-initiating glioma stem cells (GSCs) suggest that most GA-hMSCs (60%) are normal cells recruited to the tumor (Group 1 GA-hMSCs), although, rarely (10%), GA-hMSCs may differentiate directly from GSCs (Group 2 GA-hMSCs) or display genetic patterns intermediate between these groups (Group 3 GA-hMSCs). Importantly, GA-hMSCs increase proliferation and self-renewal of GSCs *in vitro*, and enhance GSC tumorigenicity and mesenchymal features *in vivo*, confirming their functional significance within the GSC niche. These effects are mediated by GA-hMSC-secreted interleukin-6, which activates STAT3 in GSCs. Our results establish GA-hMSCs as a potentially new stromal component of gliomas that drives the aggressiveness of GSCs, and point to GA-hMSCs as a novel therapeutic target within gliomas.

Keywords

Glioma stem cells; Mesenchymal stem cells; Glioblastoma; Brain Tumor; Interleukin-6; STAT3

INTRODUCTION

Although much attention is given to cell-autonomous mechanisms of tumor progression, non-cell-autonomous mechanisms, particularly interactions between tumor cells and stromal cells, are increasingly recognized as important contributors to tumor growth and resistance to therapy [1,2]. As in other cancers, glioblastoma (GBM), the most aggressive adult primary brain tumor, is maintained by a stem cell-like population of cells, called glioma-initiating cells (GICs) or glioma stem cells (GSCs), which have been the focus of intense research due their capacity for tumorigenicity, therapeutic resistance, and recurrence [3,4]. Although the cell-autonomous mechanisms of GSC growth have been extensively explored, the interaction of GSCs with the cells of the surrounding stroma remains poorly defined, despite the potential of non-GSC-autonomous mechanisms to contribute to the aggressive behavior of glioblastomas.

Compared with other cancers, the stroma of GBMs is not well understood, due to the uniqueness of the brain [1], and it is thought to be composed of reactive astrocytes, endothelial cells, and immune cells [1,2]. However, the contribution of other cell types, particularly human mesenchymal stem cells (hMSCs), has only begun to be explored [5].

Author Manuscript Author Manuscript Author Manuscript Author Manuscript

hMSCs are adult, nonhematopoietic, multipotent progenitor cells, originally isolated from the bone marrow, which are traditionally characterized *in vitro* by their plastic adherence, trimesenchymal differentiation, and expression of a panel of distinguishing surface markers [6,7]. Although bone marrow-derived hMSCs (BM-hMSCs) are the prototypical MSCs, it has recently been suggested that MSCs may reside in almost all tissues, including the brain, typically around blood vessels, as pericytes [8–10]. MSCs have been implicated in diverse physiological roles [11,12], including maintaining stem cell self-renewal and proliferation [13]. MSCs are also known for their ability to migrate to zones of tissue injury, and several studies have implicated MSCs among the bone marrow-derived cells that may be recruited into tumors [8,14–17].

We and others have shown that BM-hMSCs harvested from the bone marrow of normal volunteers and numericially expanded *ex vivo* are capable of homing to gliomas after systemic administration and can be engineered to deliver therapeutic agents to glioblastomas [18–20]. This tropism of *exogenous* BM-hMSCs for gliomas prompted us to hypothesize that *endogenous* hMSCs (i.e., hMSCs from the bone marrow or local MSCs residing in the brain) might also have a tropism for human gliomas and, therefore, may be a stromal component of GBMs that can alter the biological behavior of GSCs *in situ*. We reasoned that if this hypothesis were true, we should be able to isolate hMSC-like cells from human glioma surgical specimens and demonstrate that the isolated hMSC-like cells alter the biology of tumor-initiating GSCs. To address this hypothesis, we took a translational approach using fresh surgical specimens and now show that human gliomas harbor hMSC-like cells (referred to as glioma-associated-hMSCs (GA-hMSCs)), which can be classified into three genetic groups, and that these GA-hMSCs enhance the stemness, proliferation, and tumorigenicity of GSCs through the IL-6/STAT3 pathway. These studies identify GA-hMSCs as a heretofore unrecognized cellular component of the stroma of glioblastomas and suggest new therapeutic strategies for treating GBMs.

METHODS

Surgical brain tumor specimens

Surgical specimens taken from patients with human gliomas were obtained fresh from the operating room after participating patients granted written consent, according to an IRB approved protocol (LAB04-0001). Specimens were reviewed by a neuropathologist to assess the grade and type of tumor before assays were performed. Cell isolation procedures were typically undertaken within 4 hours of tumor removal.

Isolation of GA-hMSCs

To isolate cells resembling hMSCs, specimens were processed according to the protocol of Pittenger et al. [21], used for isolating bone marrow-derived MSCs with modifications for whole tissues. In brief, tumor specimens were washed twice in serum-free minimal essential medium–alpha (MEM-α, Mediatech, Herndon, VA), minced, dissociated, and passed through a series of cell strainers. Single cells were resuspended in standard “MSC Media,” consisting of MEM-α plus 10% certified fetal bovine serum (FBS; Lonza, Wlkersville, MA), 2 mM L-glutamine (50 U/ml, Mediatech), and penicillin/streptomycin (50 mg/ml,

Author Manuscript Author Manuscript Author Manuscript Author Manuscript

Flow Laboratories, Rockville, MD), and plated at a density of 2×10^6 live cells per 75 cm^2 flask. After 24 hours, nonadherent cells were removed by two washes with phosphate-buffered saline (PBS; Mediatech), and adherent cells were cultured until they reached confluence. Cells were trypsinized (0.25% trypsin with 0.1% EDTA) and subcultured at a density of 5000 cells/cm^2. These cells were cultured continuously through multiple passages. Cell cultures were observed with an inverted phase-contrast microscope (Axiovert 200; Zeiss, Hallbergmoos, Germany). Photographs of cells were taken with a digital camera (AxioCam MRc, Zeiss), using Xcap-Plus version 2.1 software (Epix Inc., Buffalo Grove, IL) at each passage.

Isolation of GSCs

GSCs were also isolated from surgical specimens according to the method of Singh et al. [3]. Briefly, tumor specimens were dissociated as above and resuspended in standard "Neurosphere Media," (NSC media), consisting of DMEM/F12 (Mediatech) with B27 (x1, Invitrogen), bFGF (20 ng/ml, Sigma), and EGF (20 ng/ml, Sigma). Cells were cultured as neurospheres and passaged every 5–7 days, based on sphere size.

Flow cytometry analysis

To investigate the surface expression profile, cells were trypsinized and counted in a Vi-Cell machine (Version 1.01; Beckman Coulter Inc., Fullerton, CA). Cells were washed in PBS, and pellets were resuspended in fluorescent-activated cell sorting (FACS) buffer (PBS with 10% FBS) at a concentration of 5×10^5 cells per 100 μl. These single-cell suspensions were incubated at 4°C for 30 minutes with phycoerythrin (PE)-, fluorescein isothiocyanate (FITC)-, Alexa Fluor 647-, or allophycocyanin (APC)-conjugated antibodies against human CD105, CD90, (both from eBioscience, San Diego, CA), CD73, CD34, CD45 (all from BD Bioscience, San Jose, CA) and CD133 (Miltenyi Biotech, Auburn, CA). Flow cytometry analysis was performed using a FACScalibur (BD Biosciences) flow cytometer equipped with BD CellQuest Pro version 5.1.1 software (Apple, Cupertino, CA), with 20,000 events recorded for each sample.

Differentiation protocols

Cells were differentiated into osteocytes, adipocytes, and chondrocytes using specific osteogenic, adipogenic, or chondrogenic induction and maintenance media, respectively (Lonza (Walkersville, MA), and used according to the manufacturer's suggested protocols for differentiation of human bone marrow-derived MSCs. To analyze the results of osteogenic differentiation, cells were stained with 40 mM Alizarin Red. Calcium deposits were visible within osteocytes. To analyze the results of adipogenic differentiation, cells were stained with Oil Red O. Adipogenic differentiation was verified by lipid vacuoles visible within cells. For chondrogenic differentiation, pelleted specimens were formalin fixed, paraffin-embedded, and thin sections were slide-mounted and stained for glycosaminoglycans using Safranin O staining. In each case, BM-hMSCs were used as a positive control.

Author Manuscript Author Manuscript Author Manuscript Author Manuscript

Chromosome 10 loss of heterozygosity (LOH) analysis

The multiplex polymerase chain reaction (PCR) was performed according to the standard protocol. In brief, 1–4 μl (approx. 20–100 ng) of purified genomic DNA from GSCs and GA-MSCs, in each case, was mixed with 5 μl Multi Primer Mix (PE Applied Biosystems), containing all 6 PCR primer pairs for the selected microsatellite markers. Water was added to make a final volume of 25 μl. PCR was performed using a Perkin Elmer thermocycler. The PCR conditions were as follows: after an initial 2 min denaturation step at 94°C, 30 amplification cycles were performed, each consisting of a 10 s step at 94°C, a 30 s step at 55°C, and a 30 s elongation step at 72°C. Amplification was completed with a final incubation step at 72°C for 7 min. The amplified PCR products were analyzed using the automated ABI PRISM sequencer model 310 Genetic Analyzer.

Low-pass whole-genome sequencing and copy number variant analyses

Whole-genome sequencing was performed on 10 GSCs and their matched GA-hMSC pairs and 2 unmatched GA-hMSCs using the Illumina HiSeq2000 platform. Paired-end sequencing was performed on genomic DNA fragmented to an average size of 160bp. We determined copy number variation using BICSeq [22]. The BM-hMSC was used as the common reference.

Immunofluorescence

Sections of formalin-fixed paraffin-embedded human GBM surgical specimens were deparaffinized with xylene and rehydrated through a graded alcohol series. The heat-induced antigen retrieval was carried out in a microwave for 4 min at 100% power and 15 min at 10% power, using citrate buffer at pH 6.0. Nonspecific staining was blocked by preincubation of these sections in PBS containing 5% IgG-free BSA (Jakson ImmunoResearch Laboratories) for 1 hour at room temperature. Primary antibodies used were as follows: mouse anti-CD31 monoclonal antibody 1:500 (Abcam), rabbit anti-CD31 polyclonal antibody 1:50 (Abcam), rabbit anti-CD105 polyclonal antibody 1:50 (Abcam), mouse anti-CD105 monoclonal antibody 1:50 (Abcam), rabbit anti-CD133 polyclonal antibody 1:150 (Abcam), rabbit anti-PDGFRB polyclonal antibody 1:150 (R&D), goat anti-PDGFRB 1:100 (R&D), rabbit anti-ADAM12 antibody 1:100 (Abcam). After primary antibody incubation overnight at 4°C, sections were rinsed several times with PBS and incubated with appropriate secondary antibodies at room temperature for 30 min. The secondary antibodies used were as follows: Alexa Fluor 488- or Alexa Fluor 594-conjugated donkey anti-mouse, donkey anti-rabbit, and donkey anti-goat antibodies (Invitrogen). After washes in PBS, the sections were counterstained with DAPI and mounted with anti-fade mounting medium. For antigen specificity controls, antibody diluents were used to replace either primary or secondary antibody in the corresponding incubation steps.

Coculture, cell proliferation assay, cell cycle assay and immunocytochemistry

For coculture, 24 well ThinCert™ cell culture inserts with translucent membranes and 0.4 μm pores were used. GA-hMSCs or human brain microvascular endothelial cells (hBMECs) suspended in MSC medium containing 0 (control) or 10^5 cells were pipetted into the inner side of the membrane. The cells were allowed to adhere overnight at 37°C in an atmosphere

Author Manuscript Author Manuscript Author Manuscript Author Manuscript

of 95% air/5% CO_2. Cells were washed three times and subsequently, the insert was placed in the well of 24-well plates prefilled with complete NSC medium. GSC suspensions containing 10^5 cells were added to the bottom well. Medium from upper wells was removed and fresh medium was added on each alternate day. Cocultures were maintained for 5–7 days at 37°C in an atmosphere of 95% air/5% CO_2. The Water-Soluble Tetrazolium salts (WST-1) assay was performed with the Cell Proliferation Kit I (Roche). In brief, inserts containing GA-hMSCs or hBMECs were removed and 100 μl of WST-1 solution were added to each well of a 24-well plate. After an incubation of 4 h at 37 °C in an atmosphere of 95% air/5% CO_2, 100 μl of the solution from the well were transferred to a clear bottom 96-well plate. The absorbance was measured at 450 nm. The 5-ethynyl-2´-deoxyuridine (EdU) assay was performed according to the manufacturer's protocols (Invitrogen, CA). Immunocytochemical analysis was performed according to the protocol described at www.jove.com. In brief, spheres in the bottom wells were fixed with 500 μl 4% PFA, washed twice with 500 μl PBS, and made permeable for 5 min with 500 μl 0.3% Triton/PBS. After washing with PBS, nonspecific protein binding sites were blocked with 500 μl 5% BSA in PBS for 1 h. Cells were washed with PBS and incubated for 1 h with 100 μl of different antibodies at 1:50 dilution and incubated overnight. After washes with PBS, the cells were incubated for 1 h with 100 μl Alexa 488 anti-IgG antibody (1:1000 in 1% BSA/PBS). Nuclei were counterstained with DAPI.

Animal Studies

Male athymic nude mice (*nu*/*nu*) were purchased from the Department of Experimental Radiation Oncology, The University of Texas M.D. Anderson Cancer Center (Houston, TX). Intraperitoneal (IP) injections of ketamine (100mg/kg)/xylazine (10mg/kg) were used to anesthetize animals in all experiments. All animal manipulations were performed in the veterinary facilities in accordance with institutional, state, and federal laws and ethics guidelines under an approved protocol. Intracranial and flank xenografting: Intracranial xenografts of GSCs and GA-hMSCs were implanted using a guide screw and a multiport microinfusion syringe pump (Harvard Apparatus, Holliston, MA), as previously described [18,23]. For GSC-only experiments, GSCs were cocultured with GA-hMSCs as indicated in the text, and after 5 days, only GSCs were collected and injected into the brain at the indicated number of cells in 5 μl of cell suspension. For intracranial mixing experiments, GSCs and GA-hMSCs were combined at the indicated ratios and injected intracranially (5 μl cell suspension) into the caudate nucleus via a guide screw. For subcutaneous experiments, GSCs and GA-hMSCs were combined at the indicated ratios and injected subcutaneously (100μl cell suspension) into the left flank.

Cytokine antibody array

Conditioned medium was probed for its cytokine profile using the Human Angiogenesis Array C1000 kit according to the manufacturer's instructions (RayBiotech). Briefly, membranes were blocked with a blocking buffer, and 2 ml of pooled serum samples were added and incubated at 4°C overnight. Membranes were washed, and 1 ml of primary biotin-conjugated antibody was added and incubated at room temperature for 2 h. The membranes were then incubated with 2 ml of horseradish peroxidase–conjugated streptavidin at room temperature for 30 min, and cytokine presence was detected by chemiluminescence.

Author Manuscript Author Manuscript Author Manuscript Author Manuscript

ELISA assays

The expression levels of IL6, IL8, Gro-α and MCP1 in the conditioned medium were quantified using an ELISA kit (Quantikine®, R&D Systems, Minneapolis, MN) according to manufacturer's protocol. Briefly, cells were plated at 10^5 cells/ ml in serum-free medium, and 48 hrs later the conditioned medium was collected and assayed.

Plasmids and lentivirus preparation

GP130-specific shRNA constructs were purchased from a commercial source (Open Biosystems). Lentivirus was prepared according to standard protocols with modification. In brief, lentiviruses were prepared using 293FT cells (Invitrogen) transfected with packaging vectors (psPAX2; Addgene, Cambridge, MA), envelope vectors (pMD2.G; Addgene Cambridge, MA.), and lentiviral vectors, using Lipofectamine 2000 transfection reagent (Invitrogen). For infection of GSCs, spheres were first dissociated with Accutase (Sigma), and lentiviruses were added typically 10 MOI in NSC medium containing polybrene (8 μg/ml) in a volume of 2–5 × 10^5 cells/ml, and incubated overnight. Cells were washed after 8–12h and resuspended in NSC medium containing puromycin (1 μg/ml) for selection.

Statistical Analysis

Statistical analyses were performed with GraphPad Prism. Unless specifically noted, all data are representative of >3 separate experiments. Error bars represent the SEM, were calculated using Prism, and are derived from triplicate experimental conditions. Specific statistical tests used were paired and unpaired *t* tests, and all p values < 0.05 were considered statistically significant. Graphpad Prism was used to compare two survival curves using the log-rank test.

RESULTS

CD105$^+$/CD31 cells can be identified in GBM specimens

Because MSCs are defined by *in vitro* assays [7], identifying MSCs *in situ* is difficult due to the lack of specific antibodies to the common MSC surface antigens. Nevertheless, to begin to explore whether hMSC-like cells reside in glioblastomas *in situ*, we performed immunohistochemical (IHC) analysis for CD105, the most consistent hMSC marker [7], on formalin-fixed specimens of human GBMs (SP240, SP237, and SP248). Because endothelial cells also stain for CD105, we costained for CD31, an endothelial marker. Confocal microscopy revealed a population of CD105+/CD31+ cells that were probably endothelial cells (Fig. 1a). However, we also identified CD105+/CD31- cells (Fig. 1a) that were located both around endothelial cells and distant from vessels, suggesting that hMSC-like cells reside in both perivascular sites, as pericytes [8], and in tumor tissue proper. To assess whether the CD105+/CD31- cells met other surface marker criteria for MSCs, we immunostained for CD105 and PDGFRβ, which is known to be expressed on 30–40% of BM-hMSCs *in vitro* [8,11,24]. Subsets of PDGFRβ+ cells were positive for CD105, and these CD105+/PDGFRβ+ cells resided in stromal areas both near and away from blood vessels (Fig. 1b). Importantly, CD105+ positive cells were not positive for the established pericyte marker NG2, indicating that the CD105+ cells were not mature pericytes (Fig. 1c).

Author Manuscript Author Manuscript Author Manuscript Author Manuscript

We also stained for both CD105 and CD133, a known GSC marker (Fig. 1d). Only rare colocalization of CD105 and CD133 was seen, indicating that MSCs and GSCs were distinct populations that were nevertheless present in the same niche.

Recent studies suggest that ADAM12 is a marker of activated hMSCs [25,26]. Immunostaining for ADAM12, and either CD105 or CD31, revealed a distinct population of CD105+/ADAM12+/CD31- cells, further supporting the notion that MSC-like cells exist within human gliomas *in situ* (Fig. 1e,f).

hMSCs are defined not only by CD105 expression, but also by CD73 and CD90 expression. However, antibodies against CD73 and CD90 are not effective in IHC analysis. Consequently, to further demonstrate the potential of MSCs to reside in GBMs *in situ*, we assessed fresh glioma specimens using FACS analysis for the presence of triply positive (CD105+/CD73+/ CD90+) cells before culturing. SP231, SP240, and SP262 harbored 13.4%, 1%, and 9.1% triply positive cells, respectively (Fig.1g), indicating that glioma specimens harbor cells with the surface characteristics of hMSCs.

MSC-like cells can be cultured from human gliomas

Our immunohistochemical and flow studies suggested the presence of MSCs in human gliomas, but MSCs are officially defined by *in vitro* criteria [7]. Consequently, we sought to isolate MSC-like cells from human glioma surgical specimens using the culture conditions and criteria identical to that of BM-hMSCs, which are the prototypical hMSCs [7]. We originally cultured 32 consecutive surgical glioma specimens using the same protocol used for isolating hMSCs from bone marrow. We then assayed the isolated cells using the criteria for defining MSCs established by the International Society of Cellular Therapy [7], namely: 1) adherence to plastic with spindle shape morphology; 2) positive expression of CD105, CD73, and CD90, with negative expression of CD45 and CD34; and 3) trimesenchymal differentiation into adipocytes, chondrocytes and osteocytes. We also assayed for the GSC markers CD133, and in some cases, CD15, to prove that the cells did not have markers indicative of GSCs. Of the original 32 cultures, 9 (28%) met all three criteria (Table 1, cases 1–9; and Fig. 1h–j), and 12 cultures met all criteria except that they differentiated into two mesenchymal phenotypes (Table 1, cases 10–21). Therefore, 21 (66%) specimens had triply positive surface expression and could be differentiated into multiple (>2) mesenchymal cell types. We refer to these isolated cells as glioma-associated-hMSCs (GA-hMSCs).

Of these 21 cultures, all have been passaged multiple times (doubling time typically is 72 hrs), with several maintained until passage 30 (Supplementary Fig. 1a). We analyzed a subset of these GA-hMSCs for other markers that are commonly expressed MSCs (CD146, PDGFRβ, STRO-1, CD44) and found that these GA-hMSCs expressed levels of these markers similar to the levels expressed on prototypical BM-hMSCs (Supplementary Table 1). In addition, the GSC marker CD15 was not present on tested GA-hMSCs; specifically, GA-MSC0818, GA-hMSC240, GA-hMSC100907 had 0.9%, 0.2% and 0.6% CD15 expression, respectively, and BM-hMSCs had 1.5% CD15 expression.

Author Manuscript Author Manuscript Author Manuscript Author Manuscript

GA-hMSCs are distinct from GSCs

We were interested in determining whether GA-hMSCs were distinct from GSCs. Therefore, we used the methods described by Singh et al. to isolate GSCs from our surgical specimens [3,27]. We were able to culture GSCs from five of our original 21 specimens from which we had also isolated GA-hMSCs, giving us 5 matched pairs in which GSCs and GA-hMSCs were grown from the same tumor specimen (Table 2 pairs 1–5, and marked with asterisk in Table 1). We also isolated GSCs from several other "unmatched" specimens (Table 2, Bottom).

In order to expand our pool of matched pairs, we cultured a second series of surgical specimens in order to specifically obtain both GA-hMSCs and GSCs from the same specimen. This effort resulted in another 5 matched pairs of GA-hMSCs and GSCs (Table 1: cases 22–26 and Table 2: pairs 6–10). Consistent with our original series, the GA-hMSCs from this second series met the ISCT criteria of hMSCs, as they grew as spindle shaped adherent cells, expressed high levels of CD105, CD73, and CD90, and differentiated into mesenchymal phenotypes.

When we compared the GA-hMSCs with the GSCs we found that GSCs grew as nonadherent spheroids when cultured in typical neurosphere media, consistent with previous reports. This morphology was distinct from the adherent growth of GA-hMSCs (Supplementary Fig. 1b). In addition, the GSCs typically did not express high levels of the three canonical surface markers, CD105/CD90/CD73, suggesting that they are phenotypically distinct from GA-hMSCs (Table 2). The GSCs expressed variable amounts of CD133, a marker that is frequently, but not invariably, expressed on GSCs, whereas the GA-hMSCs did not express this marker (Table 2). Although GA-hMSCs did not express CD15 (see above), 21.6% of cells in sample GSC0818 expressed this marker. Most importantly, GSCs were highly tumorigenic (as expected), whereas no GA-hMSCs were tumorigenic, consistent with their role as stromal cells. Implanting 10^6 cells from each of the original 21 GA-hMSC cultures and from the additional 5 GA-hMSC cultures into the brains of SCID mice (N = 3–5mice/cell line) did not result in tumors, in any case (Fig. 1l; Table 1 and Table 2; Supplementary Figure 1c). In contrast, implantation of as few as 10^4 GSC-cells from each of the matched pairs and the additional unmatched GSCs resulted in highly invasive tumors similar to human GBMs in all cases (Fig. 1l; Table 2, Supplementary Figure 1c). Therefore, in all 10 matched pairs, GSCs formed GBMs *in vivo* and the corresponding GA-hMSCs did not. In addition no unmatched GA-hMSCs were able to form tumors, whereas all unmatched GSCs could initiate tumors (Table 1 and Table 2). Because the culture medium of GA-hMSCs was different from that of GSCs, we determined whether growing GSCs in MSC medium eliminated the tumorigenicity of the GSCs. Although GSCs became adherent after culture in MSC medium (Supplementary Fig. 1b), the GSCs did not lose their tumorigenicity after being cultured in it (Supplementary Fig. 1c, d). Additionally, whereas GA-hMSCs (like BM-hMSCs) do not express the neural stem cell marker SOX2, GSCs robustly express SOX2 (and Musashi) and maintain this expression even when grown in MSC medium (Supplementary Fig. 1e, f). Together, these results suggest that GA-hMSCs are a stromal population of cells in GBMs and are phenotypically distinct from GSCs based

Author Manuscript Author Manuscript Author Manuscript Author Manuscript

on their *in vitro* growth characteristics, surface marker expression, tumorigenicity, and expression of neural stem cell proteins.

We next asked whether GA-hMSCs were genetically distinct from GSCs. Specifically, we were interested in determining whether the GA-hMSCs were stromal cells recruited into the tumor or whether they were stromal cells that differentiated from GSCs. We reasoned that if the GA-hMSCs were differentiation products of GSCs, then genetic alterations found in the GSCs should also be found in the GA-hMSCs, whereas if the GA-hMSCs were recruited into the tumor from non-GSC sources, they would not display the genetic changes seen in GSCs. Tumor suppressor *PTEN* is located on chromosome 10 (ch10), and deletions of losses of ch10 are common in GBM specimens. Previous work has shown that GSCs also almost invariably demonstrate loss of chromosome 10, reflecting the loss in the tumors from which the GSCs were derived [28]. In addition, the known glioma oncogene *EGFR* is located on chromosome 7, and GSCs commonly show amplification of chromosome 7, similar to GBM specimens.

As a first step in analyzing the genetic make-up of GSCs and GA-hMSCs, we assessed LOH of chromosome 10 in BM-hMSCs (as a control) and in three randomly selected paired GSCs/GA-hMSCs and in two randomly selected unpaired GA-hMSC samples, using Gene scan technology (Fig. 1k and Supplementary Table 2). As expected, BM-hMSCs showed an intact chromosome 10, consistent with their status as a genetically normal cell type. In the three paired cases, the GSC line showed loss of chromosome 10, whereas the GA-hMSCs in each case showed two chromosome 10 alleles. In addition, we could verify an intact chromosome 10 in both of the unpaired GA-hMSC samples. These results suggested that most GA-hMSCs are distinct from GSCs and do not harbor losses in chromosome 10 that are commonly seen in most GSCs.

In order to more comprehensively characterize the genetic changes in GA-hMSCs and to compare these changes with GSCs, we performed low-pass whole-genome sequencing on our 10 matched pairs of GSCs and GA-hMSCs and on two additional unpaired GA-hMSCs (GA-hMSC2–20 and GA-hMSC230) using the Illumina HiSeq2000 platform. Paired-end sequencing was completed on genomic DNA fragmented to an average size of 160bp. Reads were aligned to build Circos plots using BM-hMSC as a reference sequence. Copy number variants were identified by BICSeq [22]. An analysis of the Circos plots revealed frequent deletions and amplifications in all GSCs (Fig. 2 and Supplementary Fig. 2). In all GSCs, chromosome 10 showed frequent block deletions (Figure 2 and Supplementary Figure 2), and Chromosome 7 showed frequent amplification. Comparing the Circos plots of the GSC/GA-hMSCs pairs revealed at least three types of GA-hMSCs (Fig. 2 and Supplementary Fig. 2). In most cases (in 6 of 10 paired samples and in the 2 unmatched samples), GA-hMSCs did not show any large-scale copy number variations, and the gains and losses that were detected in the GSCs were not detected in the GA-hMSCs (Group 1 GA-hMSCs). In particular, block deletions of chromosome 10 or gains of chromosome 7 did not occur in these GA-hMSCs when compared with the GSCs, and changes in other chromosomes (e.g., deletions of chromosome 17, which harbors the p53 gene) that were present in GSCs, were not present in the GA-hMSCs in these 8 cases (GA-hMSC0818, GA-hMSC240, GA-hMSC248, GA-hMSC268, GA-hMSC280, GA-hMSC360, and unpaired

Author Manuscript Author Manuscript Author Manuscript Author Manuscript

GA-hMSC2–20 and GA-hMSC230; Fig. 2 and Supplementary Fig. 2). We interpreted these results to indicate that these GA-hMSCs were distinct from the GSCs, and because they did not harbor mutations common to GBMs, we felt that these GA-hMSCs were probably normal MSCs that were recruited into the tumor. Of note is that these GA-hMSCs were only slightly different from normal BM-hMSCs (used as the baseline comparator) (see Discussion). Two less common patterns were also seen. In one case (GA-hMSC231) the GA-hMSC was nearly identical in copy number and structural variations to the GSC (Group 2, Fig. 2). This finding indicates that this GA-hMSC most likely originated from the GSC and suggests that on rare occasions GSCs are capable of differentiating into cells that resemble MSCs. This finding is consistent with reports showing that GSCs are also capable of differentiating into other stromal cells, particularly endothelial cells, and suggests that tumor cells may be capable of shaping the cellular components of their microenvironment [29]. Lastly, three GA-hMSCs were part of a third group (GA-hMSC20, GA-hMSC262, GA-hMSC310) that showed block copy number variations that were not identical to their paired GSCs (Fig. 2 and Supplementary Fig. 2). These GA-hMSCs may represent examples of recruited normal MSC-like cells that acquired random and unique genomic alterations due to the complex genetic pressures of the tumor microenvironment and stromal "corruption" [30]. Alternatively, they may simply have differentiated from a unique unidentified GSC. Taken together, these genetic data provide evidence that although GA-hMSCs may differentiate from GSCs, for the most part GA-hMSCs are genetically distinct from GSCs and, therefore, are probably recruited into the tumor from sources independent of GSCs.

GA-hMSCs alter the biology of GSCs *in vitro*

To determine whether GA-hMSCs influence the growth of gliomas, we first employed a coculture system using transwell plates. GSCs (GSC7-2, GSC23 or GSC240) were plated in the lower wells and GA-hMSCs (GA-hMSC230 and GA-hMSC240), or normal BM-hMSCs, were placed in the upper wells, separated by 0.4μm membrane. GSC240 and GA-hMSC240 were matched pairs. As controls, GSCs were grown in NSC medium. As a second control, and to compare MSCs with other stromal cells, human brain microvascular endothelial cells (hBMECs) were placed in the upper wells. GSC spheres cocultured with GA-hMSCs or BM-hMSCs were larger and exhibited significantly increased rates of viability compared with GSCs grown with NSC medium or hBMECs (Fig. 3a). Identical results were obtained when GSCs were grown in conditioned medium of GA-hMSCs or BM-hMSCc compared with NSC medium or conditioned medium from hBMECs (Fig. 3b). Similar results were obtained using another matched pair, GSC0818 and GA-hMSC0818 (Supplementary Fig. 3a). The growth promoting effects of GA-hMSCs were independent of whether matched pairs or unmatched pairs of GSCs and GA-hMSCs were cocultured. Moreover, coculture with GA-hMSCs or BM-hMSCs significantly increased the percentage of GSCs in S-phase, based on EDU assays (Fig. 3c).

We next examined the self-renewal of GSCs using the neurosphere formation assay. GSCs were cocultured with GA-hMSC230, BM-hMSC, hBMEC, or NSC medium. After 4 days, single GSC-cells were plated in individual wells and assayed for sphere formation. After GSCs were cocultured with GA-hMSCs or BM-hMSCs, sphere formation was twice that of

Author Manuscript Author Manuscript Author Manuscript Author Manuscript

GSCs cocultured with hBMECs or NSC medium (Fig. 3d), indicating that GA-hMSCs increased GSC self-renewal. This result was seen for mismatched GA-MSC/GSC pairs and for matched paired GSC240/GA-hMSC240 (Fig 3d). Similar results were obtained using another matched pair, GSC0818 and GA-hMSC0818 (Supplementary Fig. 3b).

In NSC medium, GSCs expressed the neuronal progenitor markers Musashi-1, Nestin, and GFAP (Fig. 3e), much like SVZ type-B progenitors, which are primitive NSCs that proliferate slowly [31]. Interestingly, GSCs cocultured with GA-hMSCs or BM-hMSCs maintained the expression of Musashi-1 and Nestin (Fig. 3e) but lost GFAP, an expression pattern that is similar to that of SVZ type-C stem cells, which are rapidly amplifying cells. Consistent with these findings, the stem cell proteins SOX2 and KLF4 were upregulated in GSCs cocultured with GA-hMSCs and BM-hMSCs relative to controls (Fig. 3f).

GA-hMSCs promote GSC tumorigenesis *in vivo*

To examine whether GA-hMSCs increase the proliferation/stemness of GSCs *in vivo*, GSC7-2 or GSC23 were cocultured for 5 days with GA-hMSC230, BM-hMSC or grown in NSC medium, and 10^4 or 10^5 GSCs were implanted into the brains of mice (N =10 mice/group). The survival time of mice that were implanted with GSCs cocultured with GA-hMSC or BM-hMSC was significantly shorter than that of mice implanted with GSCs cultured in NSC medium, indicating that GA-hMSCs increased the proliferation and/or tumorigenesis of GSCs *in vivo* (Fig. 4a). These results were confirmed in an independent experiment using the matched pair GA-hMSC240 and GSC240 (Supplementary Fig. 4a).

To determine whether GA-hMSCs specifically enhance the stemness of GSCs *in vivo*, we performed limiting-dilution assays. GSCs that were cocultured with GA-hMSCs or BM-hMSCs were more likely to form tumors when low numbers of cells were implanted (100% tumorigenicity at 10^3 cells/mouse) compared with GSCs grown in standard NSC medium or cocultured with hBMECs (40% tumorigenicity at 10^3 cells/mouse) (Fig. 4b), supporting the notion that GA-hMSCs enhance the stemness of GSCs.

Next, we assessed the contribution of GA-hMSCs to the growth of GSCs when the two cell types were implanted simultaneously without prior coculture. This model assayed the direct effects of GA-hMSCs on GSCs during tumorigenesis. We injected either GSCs alone or GSCs in combination with GA-hMSCs, BM-hMSCs or hBMECs (N=6 mice/condition) into the flanks of nude mice. GSCs injected with GA-hMSCs or BM-hMSCs resulted in larger tumors and increased the frequency of tumor formation relative to injecting GSCs alone or with hBMECs (Fig. 4c; Supplementary Fig. 4b). This result was seen for both unmatched GA-hMSC/GSC pairs and for matched pairs GSC240/GA-hMSC240 and GSC262/GA-hMSC262 (Supplementary Fig. 4b, c, e).

Next we further sought to determine whether the growth promoting effect of GA-hMSC was different for GSCs isolated from the same tumor relative to GSCs isolated from different tumors. We used a flank model system and found that GA-hMSC262 increased tumor growth to a similar extent when coinjected with matching GSC262 and unmatched GSC7-2 (Supplementary Fig 4d). This result was confirmed with matched pairs of GA-hMSC240 and GSC240 (Supplementary Fig. 4f).

Author Manuscript Author Manuscript Author Manuscript Author Manuscript

We then extended these “mixing’ experiments to the orthotopic intracranial model. We mixed equal numbers of GFP-labeled GSC7-2 and GA-hMSC230 or BM-hMSCs and implanted the mixtures directly into the mouse brains. We found that mice implanted with GSC7-2 mixed with GA-hMSCs died significantly earlier than mice implanted with GSC7-2 alone (Fig. 4d). Compared with controls, tumors derived from GSC7-2 mixed with GA-hMSC230 or BM-hMSCs had higher rates of proliferation based on Ki67 staining (Fig. 4e, left), 2), showed increased expression of the mesenchymal marker CD44 (Fig. 4e, middle panel), and had larger vessels (Fig. 4e, right panel).

Increases in the mesenchymal marker CD44 in the GSCs after exposure to GA-hMSCs prompted us to investigate whether GA-hMSCs have the ability to drive GSCs to acquire a mesenchymal phenotype, as defined by Philips et al. [28]. Coculture of GSC7-2 with GA-hMSCs and BM-hMSCs increased the expression of fibronectin, CD44, TAZ, YKL40 and vimentin [28,32,33] (Fig. 4f). GSC23 and GSC240 also showed similar up regulation of these mesenchymal markers after coculture with GA-hMSCs (data not shown). Therefore, GA-hMSCs can drive GSCs to acquire a mesenchymal phenotype, which has been correlated with more aggressive behavior compared with other phenotypes [28].

IL-6 mediates GA-hMSCs effects on GSCs via the gp130/STAT3 pathway

We next investigated the molecular basis underlying the effects of GA-hMSCs on GSCs. BM-hMSCs, hBMECs and GA-hMSC230 and GA-hMSC240 were cultured for 48 hrs, and the supernatant was analyzed using a protein array. GA-hMSCs and BM-hMSCs secreted high level of GROα, interleukin-6 (IL-6), and interleukin-8 (IL-8) compared with hBMECs (Fig. 5a). ELISA confirmed these results for IL-6 and IL-8 but showed no differences for GRO-α or MCP-1 (Fig. 5b for IL-6; Supplementary Fig. 5 for others). ELISA also showed low levels of secretion of IL-6 from GSCs, including matched GSC240 (compare GA-hMSC240 to GSC240 in Fig. 5b).

In order to determine whether any of these secreted factors altered the growth of GSCs, we treated GSCs (GSC7-2, GSC23, GSC240) with recombinant purified IL-6, IL-8, GRO-α, or MCP-1 and used a colorimetric assay to measure cell viability (WST-1). Treatment of these three GSC lines with IL-6 increased the viability of GSCs, whereas treatment with IL-8, GRO-α, and MCP-1 had no effect (Fig. 5c). To further characterize the role of IL-6, GSCs were exposed to increasing doses (0–10 ng/mL) of recombinant human IL-6. All GSCs showed a dose-dependent increase in viability after exposure to human IL-6 (Fig. 5d), suggesting that IL-6 mediated the increased viability observed when GSCs were cocultured with GA-hMSCs.

To prove that IL-6 mediates the effects of GA-hMSCs on GSCs, GSC7-2 was grown in cultured medium from GA-MSC230 or BM-hMSCs, with or without neutralizing antibody to IL-6. Anti-IL-6 antibody significantly inhibited the increased proliferation of GSCs induced by GA-MSC230, whereas control IgG had no effect (Fig. 5e), establishing that IL-6 mediated the enhanced viability of GSCs.

It has been shown that IL-6 activates the JAK-STAT3-pathway [34,35], that STAT3 is phosphorylated in response to IL-6, and that STAT3 enhances cellular proliferation and

Author Manuscript Author Manuscript Author Manuscript Author Manuscript

stemness [36]. In this context, western blotting showed that coculture of GSCs with BM-hMSCs or GA-hMSCs, but not coculture with hBMECs, resulted in a significant increase in STAT3 phosphorylation in GSCs (Fig. 6a). Moreover, treatment with WP1066, an inhibitor of p-STAT3 [37], blocked GA-hMSC-mediated enhancement of proliferation and self-renewal of GSCs in a dose-dependent manner (Fig. 6b, c), further confirming a role of p-STAT3 in mediating the effect of GA-hMSCs on GSCs.

We sought to clarify the role of gp130, the coreceptor of IL6, in the interaction between GA-hMSCs and GSCs by targeting the expression of gp130 using shRNA. Two different shRNAs against gp130 were stably expressed in GSC7-2 (creating GSC7-2-gp130shRNA1 and GSC7-2-gp130shRNA2). Western blotting documented reduction in gp130 expression in both cell lines (Fig. 6d). When grown in cultured medium from GA-MSC230, both GSC7-2-gp130shRNA1 and GSC7-2-gp130shRNA2 showed significantly decreased proliferation and self-renewal (Fig. 6 e , f) relative to parental-GSC7-2, indicating that the effects of GA-hMSCs on GSCs were dependent on the gp130/STAT3 axis. Similarly, implantation of GSC7-2-gp130shRNA1 plus GA-hMSC230 or of GSC7-2-gp130shRNA2 plus GA-hMSC230 into nude mice resulted in small tumors that were similar in size to those produced by GSC7-2-gp130shRNA1 and GSC7-2-gp130shRNA2, respectively, and to GSC7-2 parental cells (Fig. 6g). These data indicated that silencing of gp130 expression in GSC7-2 significantly reduced the ability of GA-hMSC230 to augment tumor growth *in vivo*.

DISCUSSION

We show that the stroma/microenvironment of human GBMs contains heretofore unidentified MSC-like cells, called GA-hMSCs, which are phenotypically similar to BM-hMSCs, in terms of cellular morphology, surface markers, and differentiation potential, and differ from tumor-initiating GSCs with respect to surface markers, stem cell proteins, and potential for tumor formation. Importantly, most GA-hMSCs are also genetically distinct from GSCs, as GA-hMSCs do not harbor mutations commonly seen in GSCs, which suggests that GA-hMSCs are non-tumor cells recruited into GBMs, although our data also suggest that on rare occasions GA-hMSCs may differentiate from GSCs. Equally important, we show that GA-hMSCs are not mere bystanders in the GBM stroma, but instead they are capable of increasing the proliferation and self-renewal of GSCs based on *in vitro* and *in vivo* assays using both matched-pairs and unmatched GA-hMSCs and GSCs. Mechanistic studies indicate that the effects of GA-hMSCs are mediated at least in part by IL-6, which is secreted by GA-hMSCs, and which results in up regulation of p-STAT3 in GSCs.

Finding MSC-like cells in the niche where GSCs reside is unique [38]. Experimental studies using normal BM-hMSCs have implicated MSCs as stromal cells that support the growth of other solid tumors, particularly breast cancer [17]. However, the MSCs used in these studies were not directly isolated from primary tumors [17]. MSC-like cells have been isolated from human ovarian and gastric cancers [14–16], but their distinction from cancer-initiating cells has not been reported, and no study has analyzed the effects of MSC-like cells on cancer stem cells that are also obtained from patients' tumors. In this context, we show for the first time that GA-hMSCs can be isolated from human glioma surgical specimens [7]. Therefore,

Author Manuscript Author Manuscript Author Manuscript Author Manuscript

along with astrocytes, endothelial cells, and immune cells, GA-hMSCs are an important component of the microenvironment of glioblastomas.

According to our results from whole-genome sequencing and the differences in LOH patterns between matched pairs of GSCs and GA-hMSCs obtained from the same specimen, the majority of GA-hMSCs are genetically distinct from GSCs and typically do not harbor the mutations commonly seen in GSCs, e.g., losses of chromosome 10 or gains of chromosome 7 (Group 1 GA-hMSCs). This result suggests that most GA-hMSCs are either normal cells recruited to the tumor or at least are pre-existing nontumorigenic cells, similar to the stromal cells observed by Fomchenko et al. in animal models of GBM in which tumor cells and stromal cells were independently tracked [30]. This finding is consistent with the concept that MSCs are recruited into solid tumors either from the bone marrow or from local perivascular sites within the brain. The identification of relatively normal GA-hMSCs in the tumor is predicted from multiple studies that have shown that BM-hMSCs have a tropism for human gliomas and migrate/home to GBMs after intracranial or intravascular injection [18–20]. Although these Group 1 GA-hMSCs were similar to BM-hMSCs, which were used as the comparator, these GA-hMSCs harbored low-level genetic alterations that were not found in the BM-hMSCs. These differences between GA-hMSCs and BM-hMSCs may simply represent statistical variation or errors inherent to low-passage whole-genome sequencing. Alternatively, they may suggest that normal GA-hMSCs can be genetically “corrupted” due to the pressures inherent in the microenvironment of GBMs or to their interaction with GSCs. This concept of “stromal corruption” was demonstrated by Fomchenko et al. in an animal model of GBM in which cell tracing methods definitively identified non-tumor stromal cells with mutations similar to the tumor cells that pushed the stromal cell to become tumor initiating cells [30]. These animal models suggest a complex interaction between tumor cells and stromal cells that cannot be assessed by a “snap-shot” analysis of GBM stroma that is inherent to studies using human specimens, such as ours. Consistent with this complexity, in one of our specimens, we found that the cells identified phenotypically as GA-hMSCs had a genetic composition identical to the GSCs that were extracted from the same specimen (Group 2 GA-hMSCs). This result suggested that on rare occasions (~10%) it is possible for tumor cells (GSCs) to differentiate into GA-hMSCs. The capacity of GSCs to drive the architecture of the tumor environment by directly differentiating into stromal cells was shown by Wang et al., who demonstrated that GSCs from GBMs can differentiate into tumor vasculature [29]. Similarly, previous studies in breast cancer have suggested that the presence of genomic alterations similar to those observed in cancer cells may facilitate the tumor-promoting phenotype observed in tumor-associated stromal cells [39–41]. Lastly, we observed GA-hMSCs that contained genetic alterations not identified in GSCs (Group 3 GA-hMSCs). These GA-hMSCs could represent an extreme form of “stromal corruption” of normal recruited BM-hMSCs or local brain MSCs, or it could represent differentiation of a unique GSC population in the tumor. Cellular tracing studies in animal models will ultimately be required to deconstruct these potential mechanisms. Despite this complexity, our study establishes the notion that specific genomic changes are not prerequisites for the GA-hMSC phenotype.

We show that GA-hMSCs are not bystanders in gliomas. Although previous reports suggest that endothelial cells drive the growth of GSCs [42], we did not see a significant role of

Author Manuscript Author Manuscript Author Manuscript Author Manuscript

hBMECs. However, we found that GA-hMSCs have the capacity to promote GSC proliferation and stemness. We observed that GA-hMSCs' tumor promoting ability occurred in heterotopic xenografts in mouse flank as well as orthotropic xenografts in mouse brain. Interestingly, the effects were more evident in flank tumors, where GSCs were unable to form tumors without GA-hMSCs, suggesting that GA-hMSCs produce a highly permissive environment for GSC growth. Importantly, we show that the effects occur for mismatched GSCs and GA-hMSCs, as well as for matched pairs (see data for GSC240/GA-hMSC240, GSC8-18/GA-hMSC8-18, and GSC262/GA-hMSC262). Consistent with our findings Sneddon et al. [12] recently showed that organ-matched mesenchymal stromal cells permit proliferation and self-renewal of normal progenitors cells, enabling expansion of endodermal cells with retention of their developmental potential. Thus mesenchymal cells may have an intrinsic ability to maintain the stemness of tissue specific progenitor cells, a property that is exploited by cancer stem cells. Altogether the changes induced by GA-hMSCs account for the enhanced tumorigenicity seen *in vivo* and may explain the highly aggressive nature of gliomas. These results are consistent with the effects of MSCs on other cancers, including breast cancer, where they have been shown to enhance metastases [17]. Recently Ho et al. [43] reported that BM-hMSCs inhibit glioma cell growth by inhibiting angiogenesis, which directly contradicts our results and the results of publications by others [16,17,44,45]. This discrepancy may be due to the fact that Ho et al. [43] used serum-cultured glioma cells in their experiments, whereas we used patient-derived GSCs that were never exposed to serum and that probably reflect human glial cells with greater fidelity than serum-cultured cells.

Using micro-arrays, Phillips et al. [28] and Verhaak et al. [32] showed that some glioblastomas express a mesenchymal phenotype [28,42]. Although it has been assumed that tumor cells are responsible for this phenotype, because these studies did not separate stroma from tumor cells, it is possible that GA-hMSCs are at least partly responsible for global expression profiles. We observed that GSCs cocultured with GA-hMSCs expressed mesenchymal markers (vimentin, CD44, TAZ, YKL40). Conversely, our flow cytometry data suggest that the percentage of triply-positive (CD105+/CD73+/CD90+) cells varies in glioma specimens. Consequently, it is possible that the mesenchymal phenotype is due both to GA-hMSC-induced up regulation of GSC-mesenchymal genes and to the presence of GA-hMSCs in the stroma.

MSCs have been shown to drive tumor biology by the secretion of soluble proteins [46]. Consistent with this concept, we show that GA-hMSCs enhance the growth of GSCs by secreting IL-6. Although patients with malignant gliomas exhibit increased IL-6 [47], the source of this IL-6 has not been elucidated. Our results suggest that GA-hMSCs may be a major contributor of IL-6 in gliomas. In addition, by binding to its gp130-associated coreceptor, IL-6 can activate Ras-ERK, JAK1-STAT3, and PI3K [35]. We found that among these, STAT3 is a critical IL-6 effector in GSCs. Indeed, previous reports have implicated STAT3 as a driver of glioma stemness and proliferation [36]. Our results would suggest that the enhanced activation of STAT3 seen in gliomas may be due at least partly to the effects of GA-hMSCs on GSCs. Moreover, we showed that GA-hMSCs secreted factors other than IL-6 (e.g., Gro-α,IL-8). Although these factors did not alter GSC proliferation or stemness,

Author Manuscript Author Manuscript Author Manuscript Author Manuscript

it is possible that they influence other functions of GSCs. This result suggests that the repertoire of proteins secreted by GA-hMSCs may be critical to GBM biology and demands further exploration.

The importance of GA-hMSCs in GSC biology opens the exciting possibility of targeting GA-hMSCs or the IL-6/gp130/STAT3 pathway for future cancer therapies. Blocking the recruitment of GA-hMSCs or blocking the cross-talk between the GA-hMSCs and GSCs via inhibition of IL-6, gp130, or STAT3 may represent new possibilities for glioma therapy. Of interest is that we and others have exploited the tropism of BM-hMSCs for gliomas by using BM-hMSCs as therapeutic delivery vehicles of antiglioma agents [18–20]. In this approach BM-hMSCs are cultured ex vivo, engineered to secrete an antiglioma protein (e.g., Interferon-β), and delivered back into the patient. Given that GA-hMSCs and normal BM-hMSCs may promote tumor growth via secretion of proteins such as IL-6, critical to the therapeutic application of BM-hMSCs is that the normal tumor-promoting repertoire of BM-hMSCs must be altered by genetically engineering the cells to preferentially overexpress an antiglioma agent, thereby subverting the natural tumor-promoting capacity of BM-hMSCs.

Supplementary Material

Refer to Web version on PubMed Central for supplementary material.

ACKNOWLEDGMENTS

We thank Stephanie Jenkins for her assistance with preparation of the manuscript. We thank David M. Wildrick, Ph.D., for editing the manuscript.

This study was supported by grants from the National Cancer Institute CA115729 and 1P50 CA127001, The Ben and Cathy Ivy Foundation, The Broach Foundation for Brain Cancer Research, The Elias Family Fund, The M.D. Anderson Center for Targeted Therapy, The National Brain Tumor Foundation, The Collaborative Ependymoma Research Network (CERN), The Gene Pennebaker Brain Cancer Fund, the Sorenson Foundation, and the Brian McCulloch Fund to F.F.L.

REFERENCES

1. Charles NA, Holland EC, Gilbertson R, et al. The brain tumor microenvironment. Glia. 2011; 59:1169–1180. [PubMed: 21446047]
2. Lathia JD, Heddleston JM, Venere M, et al. Deadly teamwork: neural cancer stem cells and the tumor microenvironment. Cell Stem Cell. 2011; 8:482–485. [PubMed: 21549324]
3. Singh SK, Hawkins C, Clarke ID, et al. Identification of human brain tumour initiating cells. Nature. 2004; 432:396–401. [PubMed: 15549107]
4. Bao S, Wu Q, McLendon RE, et al. Glioma stem cells promote radioresistance by preferential activation of the DNA damage response. Nature. 2006; 444:756–760. [PubMed: 17051156]
5. Tso CL, Shintaku P, Chen J, et al. Primary glioblastomas express mesenchymal stem-like properties. Mol Cancer Res. 2006; 4:607–619. [PubMed: 16966431]
6. Bianco P, Robey PG, Simmons PJ. Mesenchymal stem cells: revisiting history, concepts, and assays. Cell Stem Cell. 2008; 2:313–319. [PubMed: 18397751]
7. Dominici M, Le Blanc K, Mueller I, et al. Minimal criteria for defining multipotent mesenchymal stromal cells. The International Society for Cellular Therapy position statement. Cytotherapy. 2006; 8:315–317. [PubMed: 16923606]
8. Crisan M, Casteilla L, Lehr L, et al. A reservoir of brown adipocyte progenitors in human skeletal muscle. Stem Cells. 2008; 26:2425–2433. [PubMed: 18617684]

Author Manuscript Author Manuscript Author Manuscript Author Manuscript

9. da Silva Meirelles L, Chagastelles PC, Nardi NB. Mesenchymal stem cells reside in virtually all post-natal organs and tissues. J Cell Sci. 2006; 119:2204–2213. [PubMed: 16684817]
10. Kang SG, Shinojima N, Hossain A, et al. Isolation and perivascular localization of mesenchymal stem cells from mouse brain. Neurosurgery. 67:711–720. [PubMed: 20651630]
11. Karow M, Sanchez R, Schichor C, et al. Reprogramming of pericyte-derived cells of the adult human brain into induced neuronal cells. Cell Stem Cell. 2012; 11:471–476. [PubMed: 23040476]
12. Sneddon JB, Borowiak M, Melton DA. Self-renewal of embryonic-stem-cell-derived progenitors by organ-matched mesenchyme. Nature. 2012; 491:765–768. [PubMed: 23041930]
13. Roodhart JM, Daenen LG, Stigter EC, et al. Mesenchymal stem cells induce resistance to chemotherapy through the release of platinum-induced fatty acids. Cancer Cell. 2011; 20:370–383. [PubMed: 21907927]
14. Xu X, Zhang X, Wang S, et al. Isolation and comparison of mesenchymal stem-like cells from human gastric cancer and adjacent non-cancerous tissues. J Cancer Res Clin Oncol. 2011; 137:495–504. [PubMed: 20473524]
15. Cao H, Xu W, Qian H, et al. Mesenchymal stem cell-like cells derived from human gastric cancer tissues. Cancer Lett. 2009; 274:61–71. [PubMed: 18849111]
16. McLean K, Gong Y, Choi Y, et al. Human ovarian carcinoma-associated mesenchymal stem cells regulate cancer stem cells and tumorigenesis via altered BMP production. J Clin Invest. 2011; 121:3206–3219. [PubMed: 21737876]
17. Karnoub AE, Dash AB, Vo AP, et al. Mesenchymal stem cells within tumor stroma promote breast cancer metastasis. Nature. 2007; 449:557–563. [PubMed: 17914389]
18. Nakamizo A, Marini F, Amano T, et al. Human bone marrow-derived mesenchymal stem cells in the treatment of gliomas. Cancer Res. 2005; 65:3307–3318. [PubMed: 15833864]
19. Shinojima N, Hossain A, Takezaki T, et al. TGF-beta mediates homing of bone marrow-derived human mesenchymal stem cells to glioma stem cells. Cancer Res. 2013; 73:2333–2344. [PubMed: 23365134]
20. Yong RL, Shinojima N, Fueyo J, et al. Human bone marrow-derived mesenchymal stem cells for intravascular delivery of oncolytic adenovirus Delta24-RGD to human gliomas. Cancer Res. 2009; 69:8932–8940. [PubMed: 19920199]
21. Pittenger MF, Mackay AM, Beck SC, et al. Multilineage potential of adult human mesenchymal stem cells. Science. 1999; 284:143–147. [PubMed: 10102814]
22. Xi R, Hadjipanayis AG, Luquette LJ, et al. Copy number variation detection in whole-genome sequencing data using the Bayesian information criterion. Proc Natl Acad Sci U S A. 2011; 108:E1128–E1136. [PubMed: 22065754]
23. Lal S, Lacroix M, Tofilon P, et al. An implantable guide-screw system for brain tumor studies in small animals. J Neurosurg. 2000; 92:326–333. [PubMed: 10659021]
24. Daneman R, Zhou L, Kebede AA, et al. Pericytes are required for blood-brain barrier integrity during embryogenesis. Nature. 2010; 468:562–566. [PubMed: 20944625]
25. Dulauroy S, Di Carlo SE, Langa F, et al. Lineage tracing and genetic ablation of ADAM12(+) perivascular cells identify a major source of profibrotic cells during acute tissue injury. Nat Med. 2012; 18:1262–1270. [PubMed: 22842476]
26. Steinhauser ML, Lee RT. Pericyte progenitors at the crossroads between fibrosis and regeneration. Circ Res. 2013; 112:230–232. [PubMed: 23329790]
27. Singh SK, Clarke ID, Terasaki M, et al. Identification of a cancer stem cell in human brain tumors. Cancer Res. 2003; 63:5821–5828. [PubMed: 14522905]
28. Phillips HS, Kharbanda S, Chen R, et al. Molecular subclasses of high-grade glioma predict prognosis, delineate a pattern of disease progression, and resemble stages in neurogenesis. Cancer Cell. 2006; 9:157–173. [PubMed: 16530701]
29. Wang R, Chadalavada K, Wilshire J, et al. Glioblastoma stem-like cells give rise to tumour endothelium. Nature. 2010; 468:829–833. [PubMed: 21102433]
30. Fomchenko EI, Dougherty JD, Helmy KY, et al. Recruited cells can become transformed and overtake PDGF-induced murine gliomas in vivo during tumor progression. PLoS One. 2011; 6:e20605. [PubMed: 21754979]

Author Manuscript Author Manuscript Author Manuscript Author Manuscript

31. Prestegarden L, Svendsen A, Wang J, et al. Glioma cell populations grouped by different cell type markers drive brain tumor growth. Cancer Res. 2010; 70:4274–4279. [PubMed: 20460538]
32. Verhaak RG, Hoadley KA, Purdom E, et al. Integrated genomic analysis identifies clinically relevant subtypes of glioblastoma characterized by abnormalities in PDGFRA, IDH1, EGFR, and NF1. Cancer Cell. 2010; 17:98–110. [PubMed: 20129251]
33. Carro MS, Lim WK, Alvarez MJ, et al. The transcriptional network for mesenchymal transformation of brain tumours. Nature. 2010; 463:318–325. [PubMed: 20032975]
34. Hirai H, Karian P, Kikyo N. Regulation of embryonic stem cell self-renewal and pluripotency by leukaemia inhibitory factor. Biochem J. 2011; 438:11–23. [PubMed: 21793804]
35. Kishimoto T. Interleukin-6: from basic science to medicine--40 years in immunology. Annu Rev Immunol. 2005; 23:1–21. [PubMed: 15771564]
36. Niwa H, Ogawa K, Shimosato D, et al. A parallel circuit of LIF signalling pathways maintains pluripotency of mouse ES cells. Nature. 2009; 460:118–122. [PubMed: 19571885]
37. Iwamaru A, Szymanski S, Iwado E, et al. A novel inhibitor of the STAT3 pathway induces apoptosis in malignant glioma cells both in vitro and in vivo. Oncogene. 2007; 26:2435–2444. [PubMed: 17043651]
38. Hjelmeland AB, Lathia JD, Sathornsumetee S, et al. Twisted tango: brain tumor neurovascular interactions. Nat Neurosci. 2011; 14:1375–1381. [PubMed: 22030548]
39. Moinfar F, Man YG, Arnould L, et al. Concurrent and independent genetic alterations in the stromal and epithelial cells of mammary carcinoma: implications for tumorigenesis. Cancer Res. 2000; 60:2562–2566. [PubMed: 10811140]
40. Ellsworth DL, Ellsworth RE, Liebman MN, et al. Genomic instability in histologically normal breast tissues: implications for carcinogenesis. Lancet Oncol. 2004; 5:753–758. [PubMed: 15581548]
41. Fukino K, Shen L, Patocs A, et al. Genomic instability within tumor stroma and clinicopathological characteristics of sporadic primary invasive breast carcinoma. JAMA. 2007; 297:2103–2111. [PubMed: 17507346]
42. Calabrese C, Poppleton H, Kocak M, et al. A perivascular niche for brain tumor stem cells. Cancer Cell. 2007; 11:69–82. [PubMed: 17222791]
43. Ho IA, Toh HC, Ng WH, et al. Human bone marrow-derived mesenchymal stem cells suppress human glioma growth through inhibition of angiogenesis. Stem Cells. 2013; 31:146–155. [PubMed: 23034897]
44. Rowan BG, Gimble JM, Sheng M, et al. Human adipose tissue-derived stromal/stem cells promote migration and early metastasis of triple negative breast cancer xenografts. PLoS One. 2014; 9:e89595. [PubMed: 24586900]
45. Zhang XH, Jin X, Malladi S, et al. Selection of bone metastasis seeds by mesenchymal signals in the primary tumor stroma. Cell. 2013; 154:1060–1073. [PubMed: 23993096]
46. Hall B, Dembinski J, Sasser AK, et al. Mesenchymal stem cells in cancer: tumor-associated fibroblasts and cell-based delivery vehicles. Int J Hematol. 2007; 86:8–16. [PubMed: 17675260]
47. Rolhion C, Penault-Llorca F, Kemeny JL, et al. Interleukin-6 overexpression as a marker of malignancy in human gliomas. J Neurosurg. 2001; 94:97–101. [PubMed: 11147905]

Author Manuscript Author Manuscript Author Manuscript Author Manuscript

SIGNIFICANCE STATEMENT

Using a translational approach the authors establish Glioma-Associated Mesenchymal Stem Cells (GA-MSCs) as a new, and heretofore unrecognized component of the stroma of human gliomas that drive the proliferation and promote the stemness of Glioma Stem Cells (GSCs), thereby expanding our understanding of the unique microenvironment of human gliomas, and establishing GA-MSC as a novel therapeutic target in gliomas.

Author Manuscript Author Manuscript Author Manuscript Author Manuscript

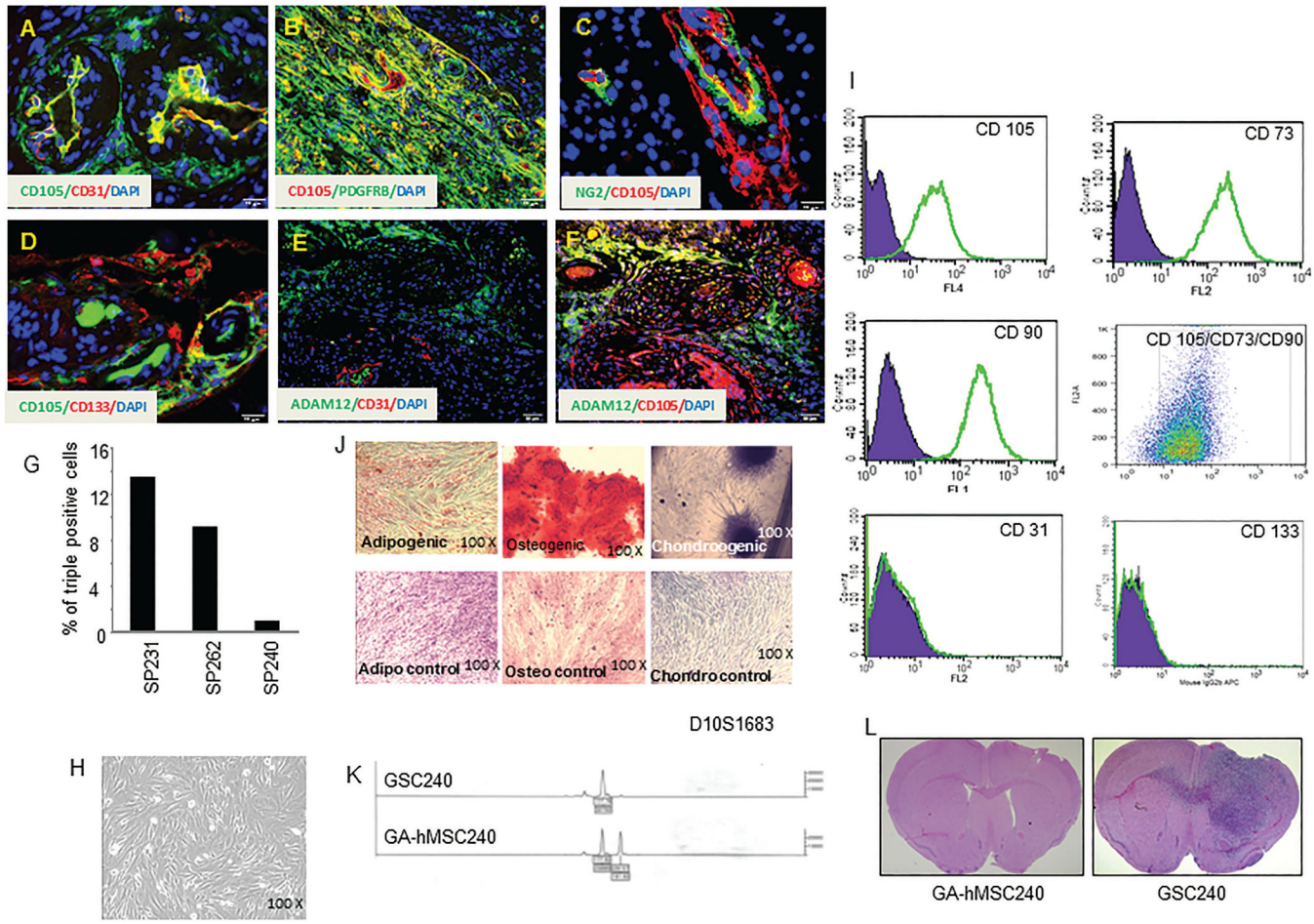

Figure 1.

Isolation and characterization of GA-hMSCs from brain tumors. **a–f**. Representative confocal immunofluorescence images of a GBM specimen showing the presence of MSC-like cells in the stroma. **a**. Double staining for the hMSC marker CD105 (green) and the endothelial marker CD31 (red) reveals CD105+ CD31- mesenchymal cells (green cells) that are distinct from the CD105+CD31+ endothelial cells (yellow cells) and that reside near the endothelial cells as pericytes and away from the endothelial cells in the tumor proper. Scale bar = 20 μM. **b**. Double staining for PDGFRβ (green) and CD105 (red), reveals significant numbers of PDGFRβ+CD105+ (yellow cells), consistent with the known expression of PDGFRβ on a subgroup of MSC-like cells. Scale bar = 50 μM. **c**. Double staining for CD105 (red) and NG2 (green) reveals that the many MSC-like cells (red) do not stain for the classic pericyte marker NG2. Scale bar = 20 μM. **d**. Double staining for CD105 (green) and CD133 (red) indicates that both MSC-like cells and GSCs exist independently within the same niche, often juxtaposed to each other. Scale bar = 20 μM. **e**. Double staining for ADAM12 (green) and CD31 (red) reveals a population of ADAM12+ cells that are distinct from endothelial cells. Scale bar = 50 μM. **f**. Double staining for ADAM12 (green).and CD105 (red) on an adjacent section shows expression of ADAM12 in CD105+ MSC-like cells (yellow cells). Scale bar = 50 μM. (for **a-f**, DAPI blue was used to stain nuclei). **g**. Graph showing the percentage of triply positive cells (CD105+/CD73+/CD90) in 3 fresh

Author Manuscript Author Manuscript Author Manuscript Author Manuscript

brain tumor specimens. Tumor specimens were dissociated into single cells and analyzed by FACS. **h**. Typical growth pattern of GA-hMSC cultured *in vitro* in MSC medium. Spindle-shaped cells are the classic morphology of MSCs. **i**. FACS analysis of typical GA-hMSC culture. Cells from specimen GA-hMSC231 were collected at passage 3 and analyzed for surface markers using antibodies to CD105, CD73, and CD90. Blue lines represent IgG control. Triple staining analysis revealed that the majority of cells were positive for all three markers. Analysis of CD34 and CD133 revealed no expression of these markers. **j**. Trilineage differentiation of GA-hMSC: GA-hMSC cells were treated with specific media for adipogenic differentiation (upper left), osteogenic differentiation (upper middle), and chondrogenic differentiation (upper right). Lower panels show staining of cells grown in MSC medium as a control. **k**. Genescan analysis of LOH of locus D10S1683 on chromosome 10 showing GSC240 with one allele (top) and its matched sample (from the same patient) GA-hMSC240 (bottom) with both alleles. **l**. Right, representative infiltrative growth pattern of typical GSCs (GSC240) grown as a xenograft in nude mouse brain. Left, matched GA-hMSCs (GA-hMSC240) did not form a tumor.

Author Manuscript Author Manuscript Author Manuscript Author Manuscript

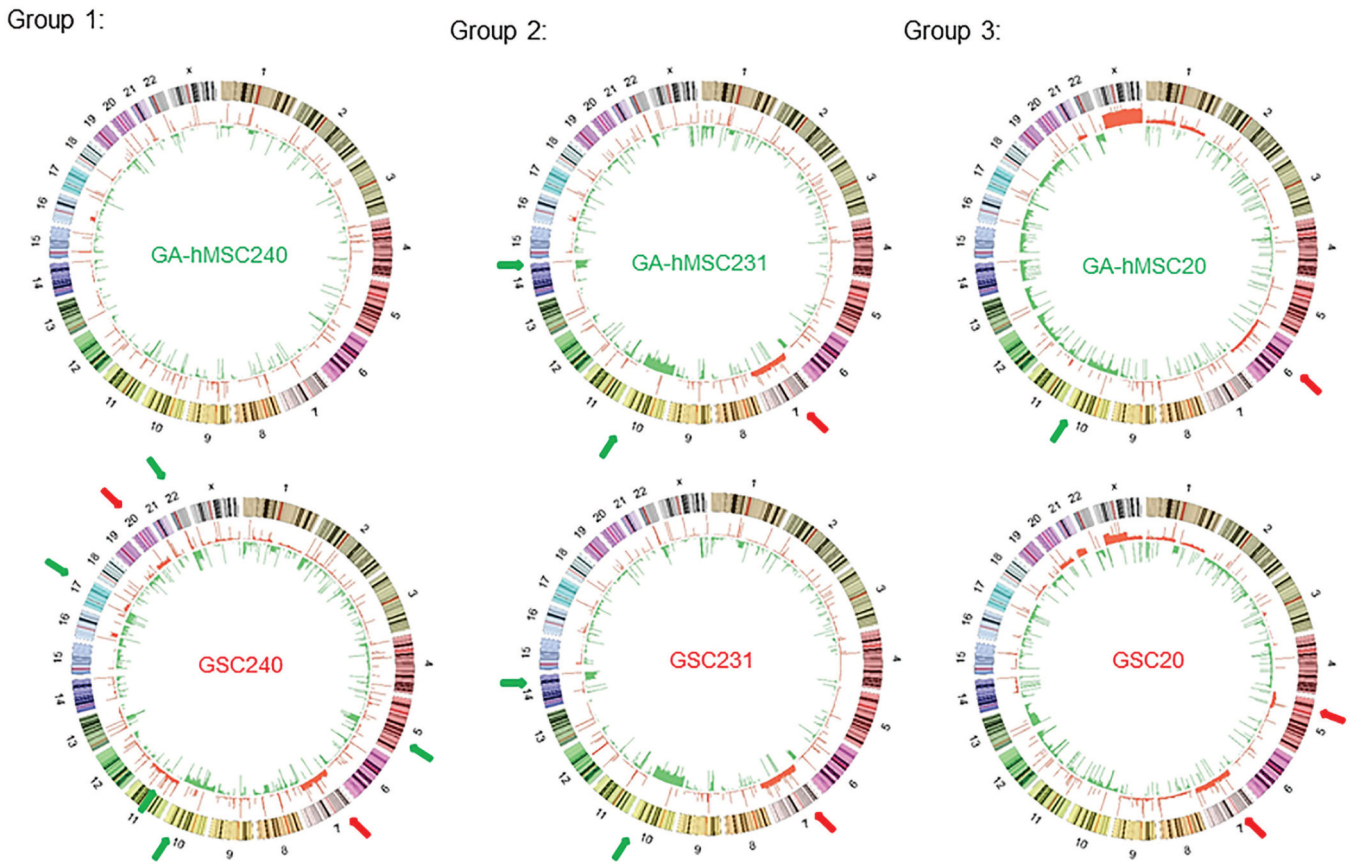

Figure 2.

GA-hMSCs are genetically heterogeneous. Representative Circos plot of genomic alterations using the copy number variants identified by whole-genome sequencing data of GA-hMSCs/GSC matched pairs and two unmatched GA-hMSCs. The outermost circle represents chromosomes and cytogenetic bands. The next inner circle represents copy number variants identified by BICSeq in which RED color indicates DNA amplifications while GREEN indicates genomic loss. Green arrows indicate major deletions and red arrows indicate major amplification events. Group 1 (example shown: GA-hMSC240/GSC240) are matched pairs in which the GA-hMSCs have minimal changes and do not harbor the deletions and amplifications seen in the GSCs (See Supplementary Fig. 2a for other pairs in this group). Group 2 (GA-hMSC231/GSC231) are matched pairs in which the GA-hMSCs and the GSCs harbor the same losses and gains. Group 3 (example GA-hMSC20/GSC20) are matched pairs in which the GA-hSMCs and the GSCs harbor different gains and losses (See Supplementary Fig. 2b for other pairs in this group).

Author Manuscript
Author Manuscript
Author Manuscript
Author Manuscript

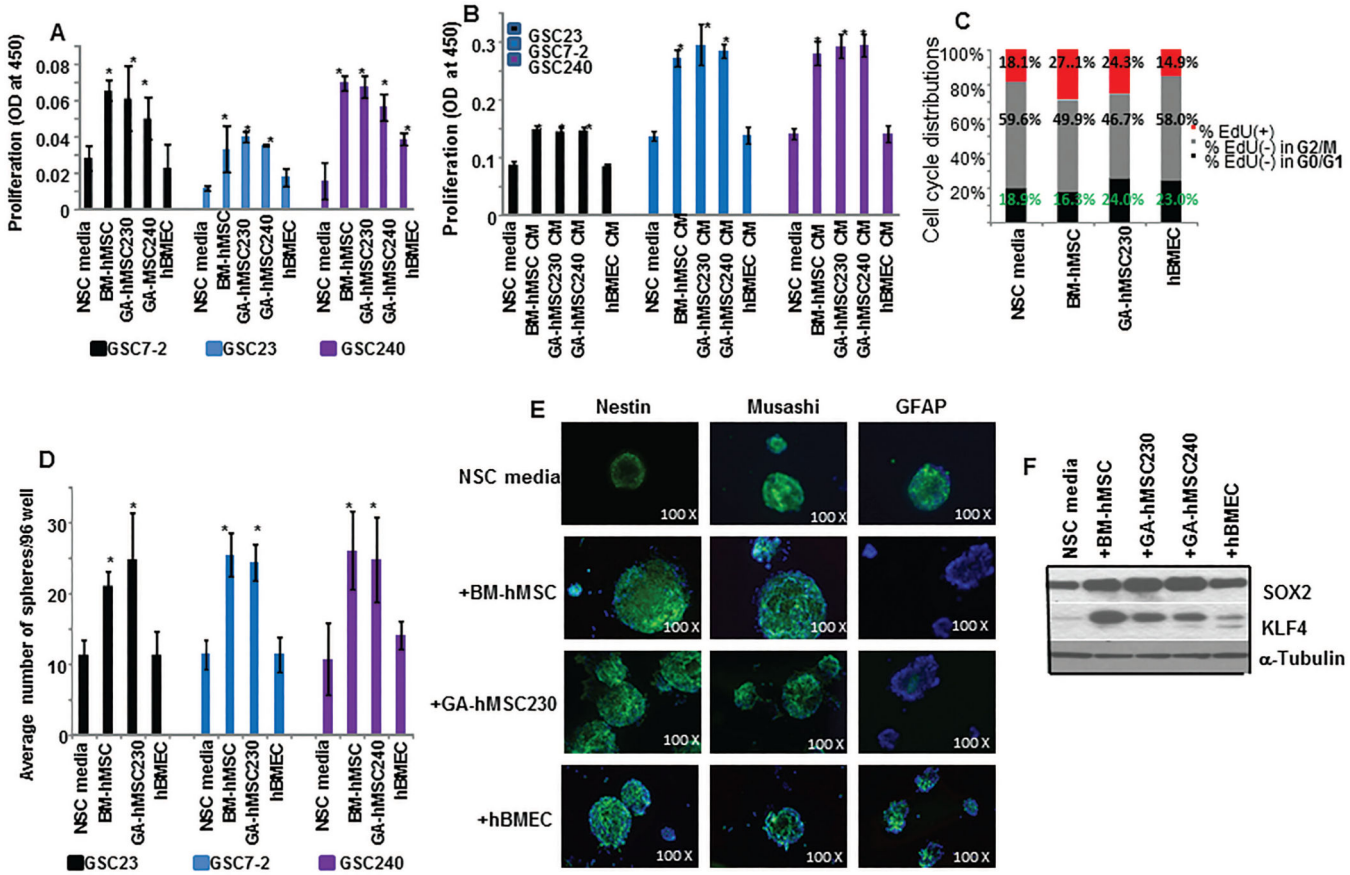

Figure 3.

GA-hMSCs promote proliferation and increased self-renewal of GSCs in vitro. **a**. GSC7-2, GSC23, and GSC240 were cocultured with NSC medium (control), BM-hMSCs, GA-hMSC230, GA-hMSC240, or hBMECs (control), and WST-1 assay was performed for cell proliferation after 5 days. Values represent mean ± S.D. * indicates p value is at least <0.04 (by paired *t* test) compared with the NSC medium group. **b**. GSCs were exposed to the conditioned medium from different GA-hMSCs, and the proliferation of the GSCs was measured after 5 days. Values represent mean ± S.D. * indicates p value <0.01 (by paired *t* test) compared with the NSC medium group. **c**. Cell cycle distribution of GSC7-2 cocultured with BM-hMSCs, GA-MSC 230, and hBMECs or grown in NSC medium alone as a control. Red bar shows percentage of cells in S-phase. **d**. Indicated GSCs were cocultured with NSC medium (control), BM-hMSCs, GA-hMSC230, or hBMECs and assayed for sphere formation from single cells plated in 96-well plates (self-renewal assay). The third graph represents the GA-hMSC240/GSC240 matched pair. Values represent mean ± S.D. * indicates p value <0.008 (by paired *t* test) compared with NSC medium group. **e**. Representative immunofluorescence photomicrographs of GSC7-2 cocultured with GA-hMSC230, BM-hMSCs, and hBMECs. Control is grown in standard NSC medium. Immunofluorescence study was performed using antibodies for nestin (left column), Mushashi-1 (middle column) or GFAP (right column). **f**. Representative western blot analyses of stem cell regulatory factor (SOX2 and KLF4) expression in GSC7-2 cocultured with NSC medium (control), BM-hMSCs, GA-hMSC230, GA-hMSC240, or hBMECs.

Author Manuscript Author Manuscript Author Manuscript Author Manuscript

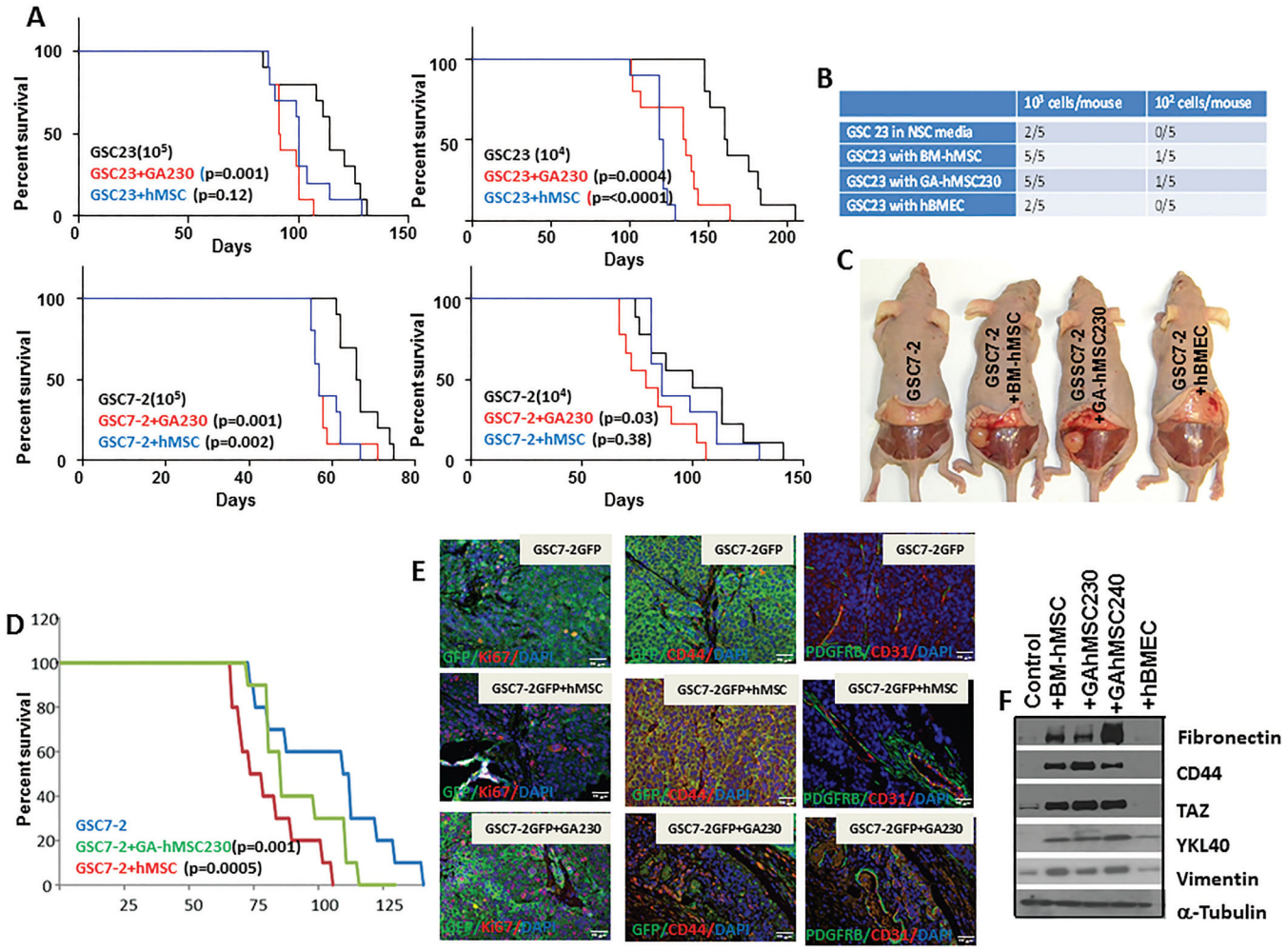

Figure 4.

GA-hMSCs enhance the growth, tumorigenicity and mesenchymal features of GSCs *in vivo*

a. Survival curves showing effects of GA-hMSCs on GSCs *in vivo*. GSC23 (top) or GSC7-2 (bottom) were cocultured with NSC medium (blue), GA-hMSC230 (red) or BM-hMSCs (green). After 7 days, GSCs (10^5, left or 10^4, right) were implanted into the brains of nude mice (N=10/group). The survival after coculture with BM-hMSCs or GA-hMSCs was significantly reduced compared with GSCs cultured in standard medium. p values (shown in parentheses) were calculated using a log-rank test. **b**. Analysis showing the increased tumorigenicity of GSCs (10^3 or 10^2 GSCs/mouse) cocultured with GA-hMSCs or BM-hMSCs. **c**. Representative mice from flank xenograft experiments in which GSC7-2 alone (10^5 cells, far left) or GSC7-2 with BM-hMSCs (10^5 cells, left middle), GA-hMSCs (10^5 cells, right middle), or hBMECs (10^5 cells, right) were injected into the left flank of nude mice. Elevating the skin reveals clear tumors only when BM-hMSCs or GA-hMSCs were injected with the GSCs. **d**. Graph showing survival of mice after GSCs were injected with GA-hMSCs orthotopically. GSC7-2GFP (10^5 cells) was mixed and coinjected with BM-hMSCs (10^5 cells), GA-hMSC230 (10^5 cells), or injected alone into the brains of nude mice (N=10/group). The survival of mice implanted with GSC7-2 mixed with BM-hMSCs or GA-hMSC230 was significantly reduced compared with GSC7-2 cells implanted alone. p

Author Manuscript Author Manuscript Author Manuscript Author Manuscript

values were calculated using a log-rank test and are shown in parentheses. **e**. Tumor specimens from animals described in section **d** were removed, fixed in paraffin, and immunostained with the shown markers. Top row shows specimens from GSC7-2 alone, middle row shows specimens from GSC7-2 +BM-hMSCs, and bottom row shows specimens form GSC7-2 +GA-hMSC230. GSCs contained green fluorescent protein (GFP), allowing for identification of tumor cells in the specimen using an antibody to GFP (green cells). Specimens were immunostained as follows: left column, GFP and the proliferation marker KI-67 (red); middle column, for GFP and the mesenchymal marker CD44 (red); and right column, for the endothelial marker CD31 (red) and PDGFR-β (green). Scale bars = 20 μM. **f**. GSC7-2 was cocultured with NSC medium (control), BM-hMSCs, GA-hMSC230, GA-hMSC240,or hBMECs (control) for 7 days, and protein was extracted. The resulting protein extracts were subjected to western blotting using antibodies against the panel of mesenchymal markers listed. α-tubulin was used as a loading control.

Author Manuscript
Author Manuscript
Author Manuscript
Author Manuscript

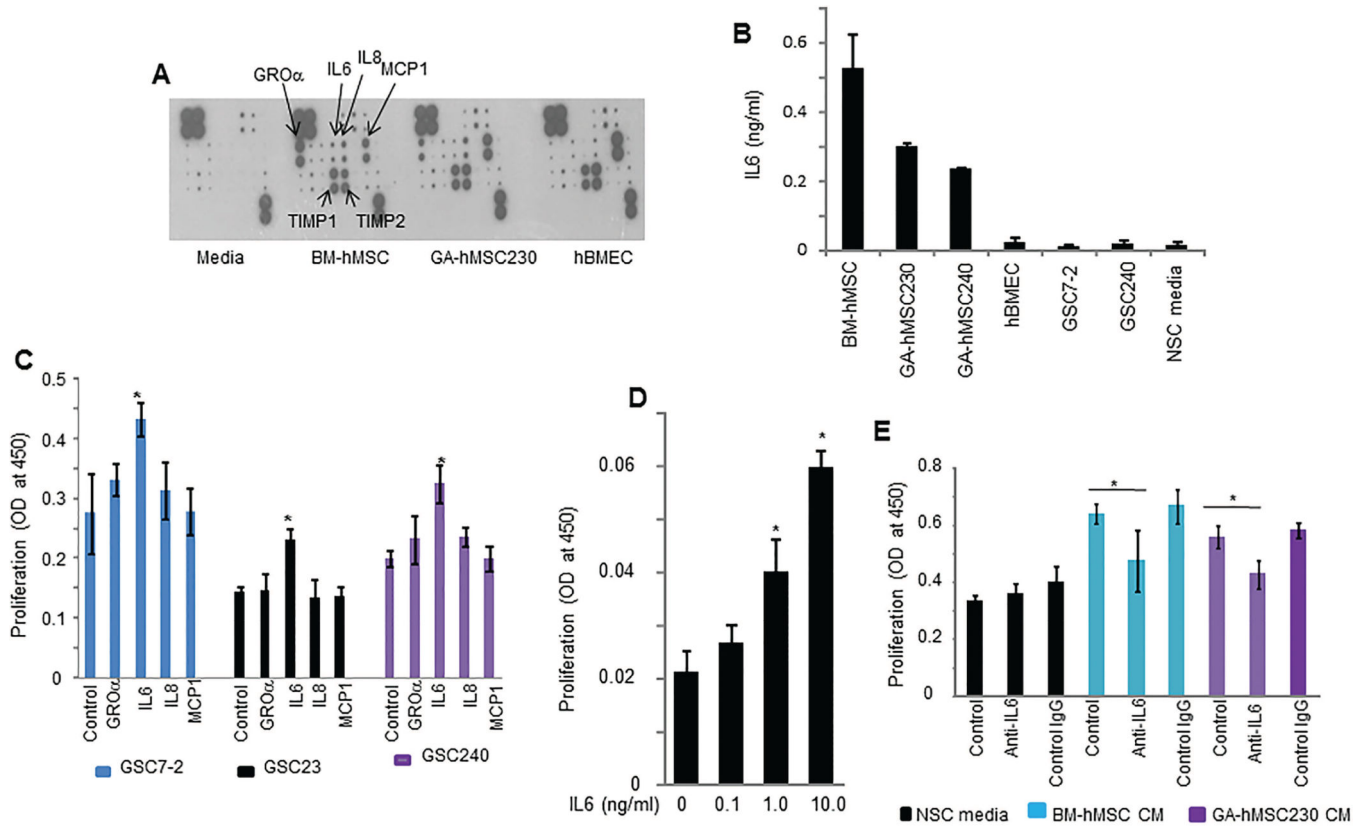

Figure 5.

IL-6 produced by GA-hMSCs promotes GSC proliferation and self-renewal. **a**. GA-hMSC230, BM-hMSCs and hBMECs were cultured in serum free medium for 3 days. The levels of various factors in the conditioned medium were measured by antibody array (Ray Biotech, GA). Each dot is a different protein (in duplicate); the intensity of the dot represents the amount of protein. **b**. ELISA for IL-6 using the conditioned medium of GA-hMSCs, BM-hMSCs or hBMECs, as well as of GSC7-2 and GSC240. Data points represent means of triplicate assays. **c**. GSCs (as shown) were grown in the presence of GROα, IL-6, IL-8, or MCP-1, each at a concentration of 50 μg/ml, and proliferation was determined using a colorimetric assay. Only IL-6 increased the proliferation of each GSC cell line. Data represents mean ± S.D. * indicates $p < 0.05$ (by paired *t* test) compared with control (NSC medium). **d**. GSC240 was grown with increasing doses of IL-6, and the viability was assessed with the WST-1 assay. Graph shows a clear dose response of GSCs to IL-6. **e**. GSC7-2 was grown in NSC medium (black), conditioned medium from BM-hMSCs (blue), or conditioned medium from GA-hMSC230 (purple). To the conditioned media, inhibitory antibody to IL-6 (5 μg/ml), or purified IgG as a control (5 μg/ml), was added. Medium conditioned by BM-hMSCs or GA-hMSC230 increased proliferation, which was reversed by the addition of the anti-IL-6 inhibitory antibody, but not by control antibody. Data represent mean ± S.D. * indicates p value < 0.05 (by paired *t* test) compared with the group treated with BM-hMSC- or GA-hMSC-conditioned medium.

Author Manuscript Author Manuscript Author Manuscript Author Manuscript

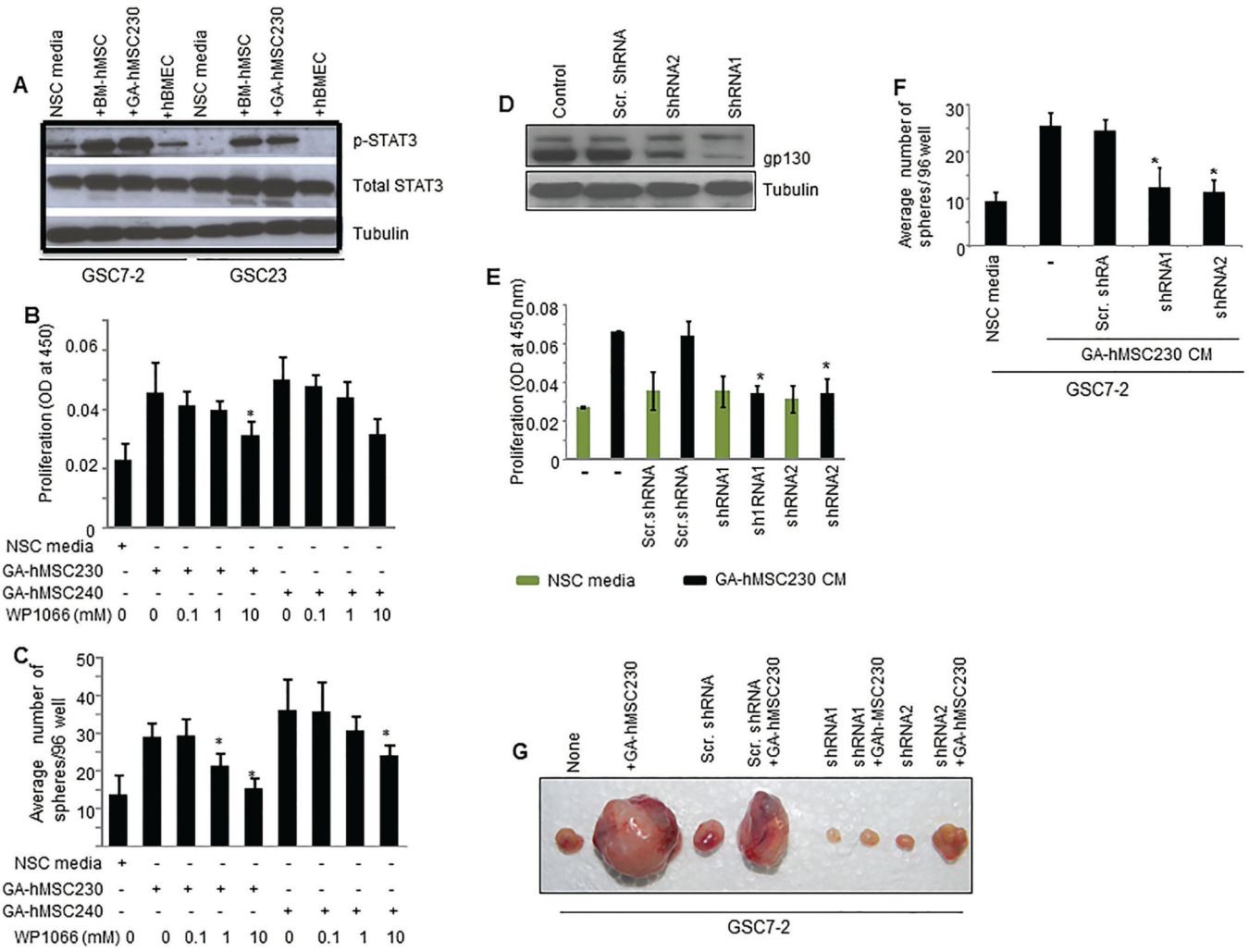

Figure 6.

Effects of GA-hMSCs on IL-6/STAT3 signaling. **a**. Western blot showing increase in phospho-STAT3 after GSC7-2 (left four lanes) or GSC23 (right four lanes) were cocultured with GA-hMSC230 or BM-hMSCs, but not after coculture with hBMECs. Control is growth in standard NSC medium. **b**. Pharmacological inhibition of the STAT3 pathway by WP1066 reverses GA-hMSC230-mediated and GA-hMSC240-mediated augmentation of GSC7-2 proliferation in a dose-dependent manner. **c**. Pharmacological inhibition of STAT3 pathway by WP1066 reverses GA-hMSC230-mediated and GA-hMSC240-mediated augmentation of GSC7-2 self-renewal in a dose-dependent manner. For **b** and **c**, data are mean ± S.D. * indicates that p was at least < 0.05 (paired *t* test) compared with the GA-hMSC230- or GA-hMSC240-conditioned medium treated value. **d**. Down regulation of GP130 expression in GSC7-2 by shRNAs, as judged by western blot results. **e**. The shRNA-mediated decrease in expression of GP130 reversed GA-MSC230-mediated and GA-hMSC240-mediated increases in proliferation of GSC7-2. **f**. The shRNA-mediated decrease in expression of GP130 reversed GA-MSC230-mediated and GA-hMSC240-mediated increases in self-renewal of GSC7-2. Data for **e** and **f** are mean ± S.D. * indicates that the p value is at least <0.003 (by paired *t* test) compared with GA-hMSC230-conditioned medium-treated wild-

type GSC7-2. **g**. The shRNA-mediated decrease in expression of GP130 reversed the effect of GA-hMSC-mediated or BM-hMSC-mediated augmentation of tumor formation of GSC7-2 in mouse flanks.

Author Manuscript Author Manuscript Author Manuscript Author Manuscript

Author Manuscript Author Manuscript Author Manuscript Author Manuscript

Stem Cells. Author manuscript; available in PMC 2016 August 01.

Table 1

Characteristics of final group of glioma-derived mesenchymal stem-like cells

	TD-MSC Cell line	Pathology	CD105[a]	CD90[a]	CD73[a]	CD73/90/105[a]	CD45[a]	CD34[a]	CD133[a]	Adipo-genesis	Chondro-genesis	Osteo-genesis	*In Vivo* Growth
1	GA-hMSC070606	GBM	95.6	97.8	65.6	64.2	0.3	nd	0.0	+	+	+	NG
2	GA-hMSC20*	GBM	52.5	99.1	84.4	46.3	0.0	nd	0.4	+	+	+	NG
3	GA-hMSC021407	GBM	33.0	98.0	52.0	22.0	0.0	nd	6.0	+	+	+	NG
4	GA-hMSC010406	GBM	96.0	9.7	90.0	9.0	0.0	0.0	0.0	+	+	+	NG
5	GA-hMSC022206	GBM	5.0	98.0	48.7	2.0	0.0	nd	0.0	+	+	+	NG
6	GA-hMSC052208	GBM	34.8	50.0	79.4	34.0	0.0	nd	0.0	+	+	+	NG
7	GA-hMSC022008	AA	99.9	54.7	99.8	53.0	0.0	nd	0.0	+	+	+	NG
8	GA-hMSC231*	GBM	99.6	92.3	99.5	92.3	0.0	nd	0.0	+	+	+	NG
9	GA-hMSC010306	GBM	99.6	4.4	99.3	4.1	0.0	nd	0.0	+	nd	+	NG
10	GA-hMSC262*	GBM	93.5	75.6	88.4	65.9	0.8	nd	0.0	+	−	+	NG
11	GA-hMSC032206	AOA	99.9	17.0	96.9	17.0	0.0	nd	0.0	+	−	+	NG
12	GA-hMSC121307	A	99.9	48.0	99.9	48.0	0.0	nd	0.0	+	−	+	NG
13	GA-hMSC081808*	GBM	99.0	31.2	99.0	28.2	0.0	nd	0.0	−	+	+	NG
14	GA-hMSC240*	GBM	98.4	17.3	98.9	15.2	0.0	nd	0.0	−	+	+	NG
15	GA-hMSC100907	AA	99.5	27.8	99.2	27.7	0.4	nd	2.2	−	+	+	NG
16	GA-hMSC092407	AA	98.8	10.8	92.5	9.7	0.2	0.0	0.0	−	+	+	NG
17	GA-hMSC102307	AA	99.7	4.5	99.8	4.0	0.0	nd	0.0	−	+	+	NG
18	GA-hMSC011906	AA	99.7	24.4	99.6	24.0	0.0	0.0	0.0	−	+	+	NG
19	GA-hMSC122806	AA	97.6	2.4	93.0	2.0	0.0	0.0	0.0	−	+	+	NG
20	GA-hMSC230	AA	93.0	86.7	99.5	67.5	0.0	0.0	0.0	−	+	+	NG
21	GA-hMSC01110	AA	99.8	27.7	99.8	24.8	0.0	0.0	0.0	−	+	+	NG
22	GA-hMSC248*	GBM	99.5	4.4	99.2	4.35	0	nd	0	−	+	nd	NG
23	GA-hMSC268*	GBM	99.24	49.38	99.86	49.26	0	nd	0	−	+	+	NG
24	GA-hMSC280*	GBM	97.8	88.73	99.9	84.54	0	nd	0	−	+	+	NG
25	GA-hMSC310*	GBM	84.17	99.95	98.28	78.94	0.13	nd	0	+	+	+	NG
26	GA-hMSC360*	GBM	98.78	72.95	99.87	71.9	0	nd	0	−	+	−	NG

Author Manuscript Author Manuscript Author Manuscript Author Manuscript

*Matching GSC isolated; nd = not determined; NG = No growth; GBM = glioblastoma; AA = anaplastic astrocytoma; A = AOA = anaplastic oligoastrocytoma;

[a]% of cells expressing marker.

Author Manuscript Author Manuscript Author Manuscript Author Manuscript

Stem Cells. Author manuscript; available in PMC 2016 August 01.

Table 2

Characteristics of GA-hMSCs and GSCs obtained from the same surgical specimen (Matched Pairs) and of Unmatched GSCs. GA-MSCs are in blue and GSCs in red.

pair	Sample	Growth Pattern	CD105/73/90[a]	CD45[a]	PDGFR-β[a]	CD133[a]	*In Vitro* Growth
1	GA-MSC20	Adherent	46.3	0.0	10.5	0.4	−
	GSC20	Spheroid	4.3	nd	0.6	2.6	+
2	GA-MSC231	Adherent	92.3	0.0	4.0	0	−
	GSC231	Spheroid	0	nd	0	0.6	+
3	GA-MSC0818	Adherent	71.9	0	34	0	−
	GSC0818	Spheroid	8.6	nd	0	0	+
4	GA-MSC240	Adherent	15.2	0.0	24.2	0	−
	GSC240	Spheroid	0.0	nd	0	43.5	+
5	GA-MSC262	Adherent	65.9	0.8	7.8	0	−
	GSC262	Spheroid	5.1		0	27.6	+
6	GA-MSC360	Adherent	78.9	0.0	nd	0	−
	GSC360	Spheroid	5.8	0	nd	36.4	+
7	GA-MSC310	Adherent	79.0	0.1	14.0	0	−
	GSC310	Spheroid	4.3	0	0	0	+
8	GA-MSC280	Adherent	84.5	0	17.6	0	−
	GSC280	Spheroid	19.4	0	0	24.4	+
9	GA-MSC268	Adherent	49.0	0	70.6	0	−
	GSC268	Spheroid	0	0	0	44.5	+
10	GA-MSC248	Adherent	4.3	0	15.7	0	−
	GSC48	Spheroid	0	0	0	0	+
unmatched	GSC7-2	Spheroid	2.9	nd	0	52.7	+
unmatched	GSC23	Spheroid	0.0	nd	nd	44.6	+

[a]% of cells expressing marker.